Aus der Klinik für Innere Medizin, CC11 Schwerpunkt Kardiologie

der Medizinischen Fakultät

Charité – Universitätsmedizin Berlin

DISSERTATION

Measuring fluid shear stress with a novel Doppler-derived relative pulse slope index and maximal systolic acceleration approach to detect peripheral arterial disease and to modulate arteriogenesis

zur Erlangung des akademischen Grades Doctor medicinae (Dr. med.)

vorgelegt der Medizinischen Fakultät Charité –

Universitätsmedizin Berlin von

Lulu Li

aus der VR. China

Datum der Promotion: 25.06.2017

Table of Contents

Abstract III
Zusammenfassung IV
Abbreviations VI
1 Introduction 1
1.1 Peripheral arterial disease (PAD) 1
1.2 Medial vascular calcification (VCm) 2
1.3 Traditional methods for assessing PAD 3
1.4 Measurement of internal flow 3
1.5 Arteriogenesis and fluid shear stress (FSS) 4
1.6 The effect of external counterpulsation (ECP) on FSS 5
2 Aim of this work 7
3 Methods 8
3.1 Patient recruitment 8
3.2 Group classifications 9
3.3 ABI measurement 9
3.4 Ultrasound-derived ACCmax and RPSI assessment 10
3.5 Angiography and Doppler assessment 12
3.6 Endovascular procedure and post-intervention surveillance 14
3.7 Practice of modulating ACCmax and RPSI-derived FSS under ECP pressure 15
3.8 Statistics 15
4 Results 17
4.1 Diagnosis of PAD 17
4.1.1 Demographic variables 17
4.1.2 Technical applicability 17
4.1.3 Haemodynamic characteristics 19
4.1.4 Diagnostic cut-off values in non-diabetic and diabetic populations, respectively 21
4.1.5 Diagnostic strategy with combination models 24
4.2 Post-revascularisation surveillance 27
4.3 The real-time dynamics of ACCmax and RPSI under ECP 28
5 Discussion 30
5.1 Validation of the Gefäßtachometer approach on peripheral arteries 31
5.2 Diagnostic application in screening PAD patients 32
5.3 Advantages of post-intervention controlling 38
5.4 The applicability of modulating ACCmax and RPSI-derived FSS under ECP pressure 39

6 Conclusion 40
Bibliography 41
Affidavit 46
Declaration of any eventual publications 47
Curriculum Vitae / Lebenslauf 48
Publikationsliste und Kongressbeiträge 49
Acknowledgement 50

Abstract

Generally, the severity of PAD is monitored over time by the ankle-brachial index (ABI); however, the disease progression of PAD in diabetic individuals is often underestimated due to frequent medial vascular calcification (VCm).

To improve the diagnostic precision of PAD for diabetic patients, two novel Doppler measurements that assess peripheral blood flow were investigated: the maximal systolic acceleration (ACCmax) and relative pulse slope index (RPSI). The feasibility of these non-invasive approaches was validated in a prospective clinical trial using a novel algorithm called 'Gefäßtachometer'.

1) Specifically, ACCmax and RPSI were evaluated in 168 patients (310 arteries measured), including 91 non-diabetic and 77 diabetic patients. The optimal threshold of ACCmax was calculated to be 444 cm/s^2 in the diabetic population, with a positive predictive value (PPV) of 96% and a negative predictive value (NPV) of 72%. The optimal threshold of RPSI was calculated to be 74 s^{-1} in diabetic populations, with a PPV of 91% and an NPV of 71%. Compared to the ABI measurements, the diagnostic PPVs increased by 22% using ACCmax and by 17% using RPSI. A logistic regression and a parallel test were conducted, which further increased the diagnostic specificity to 95% in the diabetic population.

2) Twenty-five PAD patients were enrolled one day before revascularisation, and 44 tibial arteries were measured one day before revascularisation and directly after revascularisation. The ACCmax increased from 427.83 ± 171.67 cm/s^2 to 509.30 ± 171.23 cm/s^2 ($P = 0.002$); the RPSI decreased from 82.17 ± 58.76 s^{-1} to 64.08 ± 39.65 s^{-1} ($P = 0.022$).

3) Moreover, a dynamic change of ACCmax and RPSI under different ECP treatment pressures was observed in 18 healthy volunteers. The ECP device, composed of electrocardiographic-triggered compressions of the lower extremities, has been widely applied for refractory angina pectoris. With an increase of ECP pressure from 0 to 200 mmHg, the haemodynamics of the participants responded differently on an individual basis to the increase of ECP pressure, and the maximal amplitude of diastolic ACCmax was approximately 200%.

In summary, the RPSI and ACCmax measurements provided a more predictive diagnosis than ABI for estimating the PAD status in diabetic patients. The digital translation of Doppler signals and the computer-assisted calculation of haemodynamics served as essential technical foundations for future computer-aided PAD diagnoses. These data may guide post-revascularisation surveillance and may allow for optimised and novel individual ECP treatments.

Zusammenfassung

Allgemeinen wird die periphere arterielle Verschlusskrankheit (pAVK) durch die Messung des Knöchel-Arm-Index (ABI) in Stufen eingeteilt und überwacht. Jedoch wird das Fortschreiten der pAVK bei Diabetikern häufig aufgrund von medialen Gefäßverkalkungen (VCm) unterschätzt.

Um die Genauigkeit einer pAVK Diagnose für Diabetes-Patienten zu verbessern, wurden in dieser Arbeit zwei neue Doppler-Messungen des peripheren Blutfluss durch computer-gestürzte Algorithmen (Gefäßtachometer) untersucht: 1) die maximale systolische Beschleunigung (ACCmax) und 2) der relative Pulse Slope Index (RPSI). Die Qualität dieser nicht-invasiven Messansätze wurde in einer prospektiven klinischen Studie in drei Teilschritten charakterisiert.

1) Für die oben beschriebenen Validierung der Messparameter ACCmax und RPSI wurden 168 Patienten (310 Arterien gemessen) untersucht, wovon insgesamt 91 nicht-Diabetes Patienten und 77 Diabetes-Patienten waren. Um eine pAVK bei Diabetes-Patienten zu diagnostizieren zeigte sich bei der ACCmax-Messung ein optimaler Schwellenwert von 444 cm/s^2; der positive Vorhersagewert (positive predictive value - PPV) lag hier bei 96% und der negative Vorhersagewert (negative predictive value - NPV) bei 72%. Um eine pAVK bei Diabetes-Patienten vorherzusagen lag der optimale Schwellenwert bei der RPSI Messung bei 74 s^{-1}; mit einem PPV von 91% und einem NPV von 71%. Im Vergleich zu einer ABI-Messungen erhöht sich der diagnostische Vorhersagewert PPV bei der ACCmax Messung um 22% und bei der RPSI Messung um 17%. Weiterhin wurde ein statistische Paralleltest durchgeführt, welcher die diagnostische Spezifität in der diabetischen Population auf 95% erhöhte.

2) Fünfundzwanzig PAD Patienten wurden einen Tag vor Revaskularisierung einer ACCmax und RPSI Messung unterzogen. Hierfür wurden 44 Tibialarterien einen Tag vor der Revaskularisierung und direkt nach Revaskularisation untersucht. Vor/Nach Messung stiegen die ACCmax Mittelwerte im Ergebnis von 427,83 ± 171,67 cm/s^2 bis auf 509,30 ± 171,23 cm $/s^2$ ($P = 0,002$); die RPSI Mittelwerte verringerte sich von 82,17 ± 58,76 s^{-1} auf 64,08 ± 39,65 s^{-1} ($P = 0,022$).

3) Im dritten Studienabschnitt wurde eine dynamische Änderung von ACCmax und RPSI unter verschiedenen ECP Behandlungsdruckstufen an 18 gesunden Probanden untersucht. Ergebnisse zeigten, dass ein Anstieg des ECP-Therapiedruckes von 0-200 mmHg eine individuell unterschiedliche Hämodynamik bei den Teilnehmern bewirkt. Die Erhöhung des ECP-Drucks bewirkte eine maximale Amplitude des diastolischen ACCmax von 200%.

Zusammenfassend zeigte die hier beschriebene Studie, dass die Gefäßtachometer Technik, zur Bestimmung des RPSI und ACCmax eine prädiktiver Diagnose der pAVK bei Diabetes-Patienten

besser abschätzen kann als eine klassische ABI-Messung. Die hier beschrieben Parameter zeigten auch ihren Nutzen bei der post-Revaskularisations-Überwachung und für die Bestimmung eines optimierten und individuellen ECP-Therapiedruck zur Behandlung der pAVK.

Abbreviations

ABI	Ankle-brachial index
ACCmax	Systolic maximal acceleration
ATA	Anterior tibial artery
ATP	Posterior tibial artery
AUC	Area under the curves
Bp	Blood pressure
CKD	Chronic kidney disease
CTA	Computed tomography angiography
CVD	Coronary vascular disease
DICOM	Digital imaging and communications in medicine
DM	Diabetes mellitus
ECP	External counterpulsation
EECP	Enhanced external counterpulsation
ESC	European society of cardiology
ESRD	End-stage renal disease
Fmax	Maximal frequency of the Doppler spectrum
HBP	Blood hypertension
LOESS	Locally weighted scatterplot smoothing
LVEF	Left ventricular ejection fraction
MGM	Modified geometric method
MRA	Magnetic resonance angiography
NPV	Negative predictive value
PAD	Peripheral arterial disease
PPV	Positive predictive value
PWV	Pulse wave velocity
ROC	Receiver operating characteristic
RPSI	Relative pulse slope index
T_2D	Diabetes type II
TBI	Toe-brachial index
VCi	Internal vascular calcification
VCm	Medial vascular calcification
Vmean	Mean blood velocity

1 Introduction

1.1 Peripheral arterial disease (PAD)

PAD causes a pathogenic narrowing of the arteries, and it may lead to ischemic pain, lesions or amputations when the balance between the blood flow and the metabolic demands of the lower limbs fails[1]. Ischemic pain usually results in walking-related intermittent claudication in the calf muscles or other lower extremities, which is alleviated with rest. Since 2000, the global prevalence of peripheral arterial disease (PAD) has drawn more and more attention. The Rotterdam study, the most comprehensive epidemic study, documented that intermittent ischemic pain existed from 1% in those 55–60 years of age to 4.6% in those 80–85 years of age[2].

While a large number of elderly patients have been diagnosed with PAD, only a minority experience intermittent claudication. The most influential cross-sectional survey until now showed that the prevalence of asymptomatic PAD was 8.0% among the general population of 55–74 years old, compared to prevalence of 4.5% of intermittent claudication[3]. As defined by the ankle-brachial index (ABI) of ≤ 0.90 in either leg, 16.9% of men and 20.5% of women with the age of older than 55 years have been diagnosed with PAD, independent of the symptoms of intermittent claudication[2].

The risk of amputation becomes substantial when resting pain, ischemic ulceration or gangrene occur[1]. An epidemiologic study in 2015 revealed that in-hospital amputation rates progressively increased from 0.5% among patients with claudication or resting pain to 42% among patients with necrosis and gangrene[4]. The amputation rate is particularly high among patients with diabetes complications, and a 22.8 fold increase compared to amputations in the non-diabetic population has been shown[1, 5]. Moreover, critical limb ischemia patients have a risk for all-cause and CVD mortality that is over three times higher than for patients who only experience intermittent claudication[6].

The main risk factors for PAD are similar to those for coronary and cerebrovascular disease: smoking and diabetes[7]. A higher percentage of men than women suffer from PAD. Due to the worldwide demographic shift in populations, it is probable that PAD will become progressively prevalent in the future.

In general, diabetic patients suffer from PAD without ischemic symptoms most often, but they have demonstrated infrapopliteal arterial lesions and medial vascular calcification (VCm)[8-13]. These unique pathogenic factors make it difficult to detect PAD in diabetic populations, which

results in late treatment[14]. Furthermore, as PAD is a strong predictive factor for succeeding CVD events, such as myocardial infarction, late detection of PAD also brings risks for patients due to the late consciousness of potential CVD[15].

1.2 Medial vascular calcification (VCm)

The coexistence of VCm and PAD is common. Arterial calcification limits vessel walls' mechanic expansion under blood flow and thus affects the blood flow dynamics in the affected vasculature.

As mentioned before, diabetic patients are more likely to be affected by VCm and demonstrate as 'asymptomatic PAD'. While a proportion of asymptomatic PAD patients could be readily confirm through ABI[3, 16], patients suffered from VCm cannot be detected by ABI due to uncompressible arterial walls.

The most common risk factors for VCm are diabetes type II (T_2D) and end-stage renal disease (ESRD)[17]. The rate of newly diagnosed T_2D patients suffering from VCm was 17%[18], and this rate was as high as 41.5% among patients with long histories of T_2D[19]. The cases of VCm in ESRD patients are common, and the prevalence is around 27%[17]. Generally, patients suffering from VCm are young and have less conventional risk factors for atherosclerosis[20].

In progressed stages of VCm, the deterioration of the elasticity of arterial walls is paired with a progressive loss of peripheral tissue perfusion, eventually leading to arterial flow stasis[17]. On the other hand, in cases of VCm complicated with atherosclerosis, VCm would prevent compensatory remodelling which should have occurred due to atherosclerosis, and thus obviously accelerates the progression of the atherosclerotic disease[17]. Lanzer et al. proposed that ring-like calcifications are potentially responsible principles for the poor prognosis of VCm, through decreasing propulsion of the anterograde blood flow and decreasing arterial adaptation to haemodynamic alterations, noxes and senescence[21,22].

Conventional X-rays or ultrasounds provide access to VCm. The measurement of pressure wave velocity as well as microcirculatory and endothelial function tests also allow for the assessment and full functional specification of VCm; however, current diagnosis approaches for detecting VCm fail to meet clinical needs because they are time-consuming and have limited diagnostic accuracy. Standardised laboratory tests that can detect VCm are urgently needed.

1.3 Traditional methods for assessing PAD

The detection of PAD is primarily achieved by measuring ABI. Taking the lower blood pressure value of two tibial arteries as the numerator and the higher blood pressure value of bilateral brachial arteries as the denominator, their ratio is defined as ABI. An ABI ≥ 1.3 indicates non-compressible, calcified arteries. In the cases of convincing symptoms but a normal resting ABI, a repeat ABI, following exercise, can identify significant PAD.

ABI has been considered as an easy and reliable method to screen for PAD; however, for diabetic patients, the ABI measurement often underestimates the presence of the PAD as well as the severity of PAD because diabetic patients are much more likely to suffer from VCm, which leads to false higher ABI values[23]. Vascular calcification does not exclude occlusive lesions; contrarily, these two conditions have been shown to coexist in 60%–80% of cases[24].

In VCm cases, since VCm is less likely to affect the digital arteries, the toe-brachial index (TBI) is theoretically more sensitive than ABI in detecting PAD among diabetic patients. The TBI measurement is defined as toe blood pressure divided by brachial blood pressure. A TBI ≤ 0.7 is indicative of significant PAD; however, there have been concerns regarding the diagnostic accuracy of TBI in the literature, which has been limited until recently[25]. Some researchers have claimed that TBI has superior sensitivity than ABI in the case of diabetic neuropathy[26]. While other researchers have observed lower sensitivity and specificity of TBI compared to ABI in diabetic populations[27]. Therefore, the convince about the performance of TBI is still conflicting until now[28].

In addition, surveillance after revascularisation is another disadvantage of ABI because the accuracy of ABI values in predicting symptom relief or failure of revascularisation is limited[24]. As concluded by Decrinis et al.[29], an ABI increase of 0.10 predicted the relief of stenosis with a sensitivity value of 79% and a specificity rate of 92%; while an increase of less than 0.1 of ABI makes it difficult to differentiate between graft failure and other lesion progression related to PAD[30]. In summary, ABI alone is not sufficient in clinical practice for screening tests or for surveillance after revascularisation, and a novel method with less dependence on the vascular wall alteration and a better reliability after revascularisation is needed.

1.4 Measurement of internal flow

The measurement of internal flow using the Doppler method is less dependent on vascular wall alteration, but the current Doppler procedures are complex and time-consuming. In 2010,

Tongeren et al. announced a breakthrough in a diagnostic method for PAD and asserted that Doppler-derived maximal systolic acceleration (ACCmax) could serve as an objective assessment for stenosis-induced deceleration in distal tibial arteries[31]; however, only early systolic curves were analysed in their study, and the overall haemodynamic changes during one complete heart circle were ignored. Moreover, they failed to discriminate between different waveforms of Doppler signals and thus different stages of PAD. Similar to this breakthrough, in 2010, Buschmann et al.[32] derived the first-order derivative of red blood cells ($\Delta v/\Delta t$) and claimed that the quotient maximal derivative/mean velocity, expressed as relative pulse slope index (RPSI), was significantly lower in veins than in arteries and could be used as a specific parameter to detect arterial flow patterns. Therefore, it was hypothesised that the decreasing pulsatility detectable by RPSI could be a factor used in diagnosing PAD. Moreover, the employment of mean velocity takes the overall haemodynamic changes during one complete heart beat into account and thus is promising in differentiating between the different stages of PAD.

1.5 Arteriogenesis and fluid shear stress (FSS)

Based on the relations between haemodynamic characteristics and vascular remodelling processes, another prospective approach for assessing ACCmax and RPSI is computing haemodynamic stimuli and thus predicting the vascular remodelling process. The initiation of both remodelling processes – atherosclerosis and arteriogenesis – is induced by the same haemodynamic stimuli, caused by fluid shear stress (FSS). FSS is named as the tangential frictional force of the blood flow upon the unit area of endothelial wall [N/m^2 or Pa][33]. A low local FSS indicates enlarged plaques and lumen narrowing[34, 35], while an appropriate FSS leads to arteriogenesis[36] and reduces the negative effect of atherosclerosis[37].

Within blood flow, adjacent layers of fluid slide parallel to each other with different velocities. It produces a distortion of the fluid internal surface, which is defined as shear strain or shearing. For a Newtonian fluid, the stress generated by the fluid in resistance to the shear is proportional to the strain rate or shear rate[38-40] multiplied by a viscosity constant. Shear stress uses the same units as force per surface area, namely, Pa or N/m^2. The simplified estimation of FSS(τw) was expressed as:

$$\tau w = \mu * \gamma ,$$

where μ and γ represent blood viscosity and shear rate. Shear rate refers to the rate at which a

progressive shearing distortion is exerted on material substance. The shear rate of a Newtonian fluid flowing is defined as:

Shear rate（γ）=8*v/d,

where d represents the internal diameter, v equals to the time-averaged flow velocity[41], so that the unit of measurement for shear rate is s^{-1}.

Therefore, FSS（τw）can be determined as the following equation[42]:

$\tau w = \mu * (8v / d)$.

While shear stress in human studies was previously estimated based on time-average velocity, real FSS models and thus arteriogenesis were recently found to be more complex[43-46]. For physical conditions, the triphasic signal is characterised as a rapid forward blood flow during the systole phase, an initial backward blood flow in the diastole phase and then a gradual reverse of the flow during the late diastole phase[41]. This pulsatile blood flow induces two distinct shear stimuli: an extreme increase of shear rate in the initial systolic phase due to blood acceleration and then a steady shear component. For pathological conditions, several other investigations have revealed that in addition to time-averaged velocity[47, 48], retrograde flow and flow turbulence[49-51] influence arteriogenesis. Hence, new parameters that can evaluate FSS by using both a time-derivative and a time-average are urgently needed.

Based on the mathematic models of FSS, ACCmax is proportional to the maximal positive alteration in FSS. Additionally, for a given vessel diameter, RPSI is proportional to the quotient of the maximal positive alteration in FSS and the time-averaged FSS. Theoretically, the strongest pulsatile signal is expressed by the sharply increasing acceleration during early systole, which could be assessed using ACCmax. RPSI was demonstrated to be a specific parameter to detect arterial flow, and RPSI also considered the time-average velocity information.

1.6 The effect of external counterpulsation (ECP) on FSS

As the roles of FSS in remodelling processes are proven to be significant, artificially modulating FSS is a promising approach that could benefit PAD patients. There is emerging evidence that artificially increasing FSS could cause vasodilation, could lower peripheral resistance and could increase perfusion[36, 37, 52-54]. In animal-based experimental research studies, current animal models of arterial occlusion and collateral growth in the hind limb have provided a basis to

measure haemodynamic forces and to identify primary collaterals. However, due to disintegrated methodologies, different target populations and a lack of analogous pathological backgrounds, scholars working with patient-based measurements have not yet achieved a widely accepted method that can be used to modulate FSS and collateral growth.

The external counterpulsation (ECP) device has been widely applied for refractory angina pectoris. The ECP device is composed of three electrocardiographic-triggered compressions of the lower limbs. Three pairs of cuffs are applied separately on the calves and the upper and lower thighs. Inflation is induced in the early diastolic phase in the sequence of lower thighs, upper thighs and calves. Deflation is triggered rapidly at the beginning of the systole phase in the sequence of calves, upper thighs and lower thighs. During the diastolic phase, more venous blood returns, and thus diastolic blood pressure increases. In the systolic phase, the rapid decrease of compressions reduces vascular resistance. The special adaption of coronary blood flow under ECP showed that diastolic flow increased, while systolic flow decreased[55]. However this treatment only made sense, when physiological pressures were used, rather than potentially high pressure such as with Enhanced External Counterpulsation (EECP). In 2010, Buschmann et al. [36, 37] revealed the pro-arteriogenesis effect of FSS under ECP treatment. The ease of regulating ECP pressure makes it a creative intervention practice for identifying and modulating FSS.

The Doppler-derived ACCmax and RPSI is a real-time approach that is easily implemented during ECP treatment. By combining the measurement of ACCmax and RPSI with the ECP technique, a promising, novel approach to modulating FSS and thus optimising its pro-arteriogenesis effect is being developed.

2 Aim of this work

Because ACCmax and RPSI demonstrate pulsatility and could identify the value of shear stress, the aim of this study was to detect PAD using ACCmax and RPSI and to modulate ECP pressure by optimising FSS-related ACCmax and RPSI parameters.

For this purpose, there were three sub-tasks:

Sub-task (1): to calculate the cut-off values of ACCmax and RPSI to detect PAD, especially in diabetic populations;

Sub-task (2): to observe the changes of ACCmax and RPSI after balloon or stent implantation;

Sub-task (3): to monitor the dynamic changes of ACCmax and RPSI under ECP intervention.

3 Methods

All participants were informed of the study protocol, and the study was approved by the Charité ethic council (EA1/146/12). The study followed the guidelines of the Declaration of Helsinki and the institutional ethics regulations.

3.1 Patient recruitment

In the first part of the study, which was from June 2011 to December 2014, more than 600 patients who were referred to the vascular laboratory for suspicious PAD or for controlling with an established PAD history were screened. The patient inclusive criteria were:

- ≥ 50 years old
- reference of angiography or Doppler evaluation available within 6 months
- had at least two of the following risk factors:

  hypertension

  hypercholesteremia

  diabetes

  coronary artery disease

  Patients were excluded for:

- lower limb disability
- thrombosis within the last 6 months
- severe heart insufficiency (LVEF < 20%)
- arrhythmia (e.g. atrial fibrillation)
- being involved in other clinical studies

Based on these criteria, 168 participants were enrolled in the first part of this study. They were separated into four sub-groups: controls (without PAD or diabetes), diabetic, PAD and PAD

complicated by diabetes. All patients underwent ABI measurements using the standard ultrasound technique. In addition, patients with an abnormally higher ABI value were sub-classified into the VCm group, regardless of PAD history or diabetic history.

In the second part of this study, 25 PAD patients with or without diabetes who had undergone an elective revascularisation were recruited. None of them suffered from lower limb disability, new thrombose, severe heart failure LVEF < 20% or arrhythmia. The study assessments were performed one day before intervention and one day after intervention for intra-individual comparisons.

The third part of this study was a pilot study. Eighteen young (< 25-years-old) and healthy volunteers underwent a one-time ECP treatment. They did not have a CVD history, PAD history or diabetic history.

3.2 Group classifications

To evaluate the ideal diagnostic cut-off values of blood acceleration (ACCmax) and RPSI, the first part of the study was conducted in three steps:

First, to identify the threshold, 73 samples in the non-diabetic group were estimated to be needed. Specifically, this included 40 artery records from PAD patients and another 40 records from age-matching healthy participants. With these values, ROC curves could be examined while sensitivity, specificity, positive predictive value (PPV) and negative predictive value (NPV) could be calculated.

Second, to compare the diagnostic performance between RPSI and ACCmax, 148 samples from the non-diabetic group were needed, including 75 pathological artery records and 75 age-matching healthy artery records.

Third, to evaluate the diagnostic performance of ACCmax and RPSI in diabetic populations, a similar number of examples were required, which included 75 artery records without VCm and a corresponding 75 artery records with VCm.

3.3 ABI measurement

The ABI measurement was conducted after 5 minutes of resting in a supine position. Blood pressure was taken from the arms and ankles and was calculated by sphygmomanometry with an 8-MHz Doppler probe and a 12-cm cuff. From each side of the lower extremity, the lower one of either ATA pressure or ATP pressure was taken as Pleg. Otherwise, blood pressure was assessed

from both sides of arm, and the higher one was taken as Parm[56, 57]. ABI was calculated as the following equation:

ABI = Pleg/Parm.

We could evaluate ABI values as followings:

- ABI < 0.9 was ABI test positive, in which ABI < 0.4 was severely decreased ABI values and 0.4 ≤ ABI < 0.9 was mild to moderately decreased ABI;
- 0.91 ≤ ABI < 0.99 was borderline positive;
- 0.99 ≤ ABI < 1.3 was normal ABI;
- ABI ≥ 1.3 was VCm[4].

3.4 Ultrasound-derived ACCmax and RPSI assessment

After the ABI measurement, patients resting in supine positions underwent ultrasound examinations of the distal tibial arteries, which were approximately at the same anatomic level as the ABI examination. The US unit (Philips, HDX 11, Germany) was used with an L12-3 MHz transducer, and the same transducer was used for all subjects to maximise statistical power. During each examination, two techniques were used to minimise the variability. Firstly, imaging of the arterial wall was extended across the entire plane, without zooming. Secondly, the thickest vessel walls were observed. These two adjustments were normalised to reduce estimation-variability. At the same time, the general settings of the ultrasound machine were also standardised. The beam-vessel angle was optimised to be less than 60° to minimise the likelihood of skewing the frequency spectrum. The sonographer was unaware of clinical findings and ABI values. After initially scanning the distal tibial arteries longitudinally, the pulsed-wave mode was utilised to obtain the haemodynamic parameters. To be statistically comparable with ABI values, the artery that contributed to the ABI values was examined for ACCmax and RPSI in each leg, and double examinations were undertaken to ensure reproducibility.

The definition of ACCmax was taken from previous studies[31] as the maximal slope of the velocity curve in the early systolic phase. Instead of visually determining the maximal slope, duplex data was exported through one CE-certified and MPG-compliant Audio output (CE 0086, SN 1078496) (**Figure 1**), and the ACCmax was calculated using a computational algorithm of MATLAB following the steps below (**Figure 2**):

1) Obtaining sample Doppler curve images in 15 seconds;

2) Importing Doppler curves, selecting the systolic phase and contouring the edge of the Doppler curves using the modified geometric method[58];

3) Computing the collective velocity curves, by calculating the average velocity values at each relative second;

4) Determining the maximal slope with a differential equation:

$$ACC_{\max} = \max(\frac{\Delta v}{\Delta t});$$

5) Obtaining the mean blood velocity (Vmean) by calculating the average of all collected instantaneous blood velocity curves using the formula below in which time (t) refers to one integrate pulse:

$$V_{mean} = \frac{1}{n} * \sum_{n} V(t);$$

6) Calculating RPSI with the equation[32]:

$$RPSI = \frac{ACC\max}{Vmean}.$$


Figure 1 Apparatus used for a series assessment, including an ultrasound transducer, USB digital transfer and calculation program with Matlab (developed by Robert Paschke, Exist Company, Berlin).

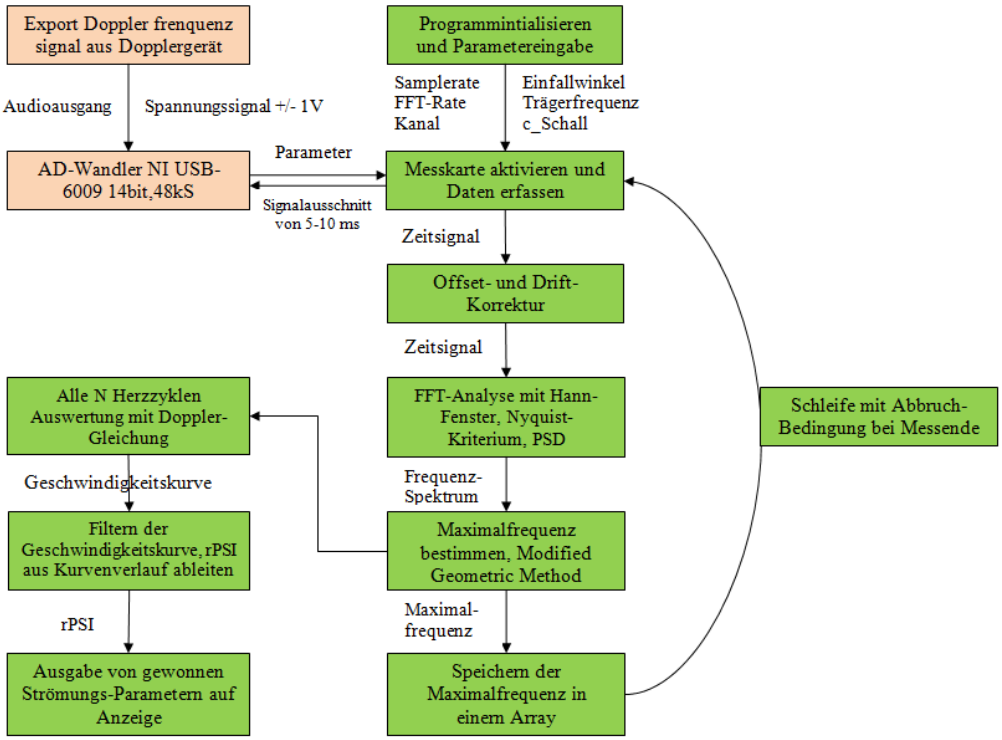

Figure 2 A summary of Matlab methods (developed by Robert Paschke, FirstFlow Company, Berlin). The image output of the system includes one 15s real-time velocity-time curve and digitising one Ensemble-curve with an average method. The velocimetry indices were obtained through the ensemble curve: $RPSI_{Ensemble} = \frac{\overline{ACC\max}_{Ensemble}}{Vmean_{Ensemble}}$

An example of the velocity profile of a normal healthy subject is shown in **Figure 3**.

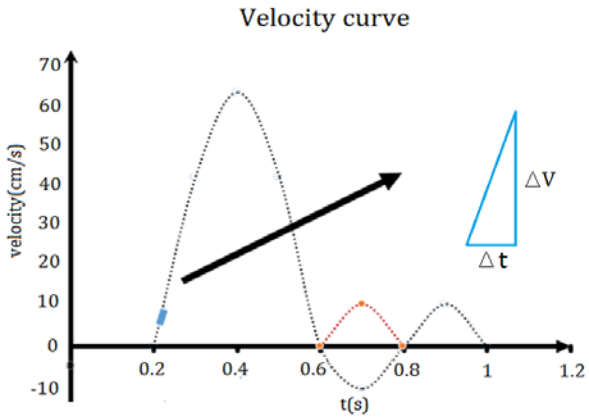

Figure 3 An example of the velocity profiles and the calculation of ACCmax on this curve.

3.5 Angiography and Doppler assessment

Patients' angiogram data were re-evaluated using quantitative analysis software (Sanders Data Systems, USA). Specific features of the SDS include 2-point user-defined path line (centre-line) identification, arterial contour detection using a minimal cost matrix algorithm and a reference vessel diameter. The minimal lesion diameter was used to calculate the percent of diameter

stenosis relative to the reference vessel diameter of the lesion of interest. The lesions were located, and the degree of stenosis was graded for each patient[59,60].

For patients with Doppler examination documents, the evaluation procedure was much simpler[59,61, 62]. The diagnosis criteria for stenosis were extensively described using diameter reduction, a qualitative waveform analysis and PSV ratios of proximal Vmax relative to distal Vmax, as well as the presence of spectral broadening (**Table 1**). In addition, high-resistance waveforms indicated a lesion proximal to the occlusion without collateral vessels. Conversely, a continuous forward diastolic flow was present in the proximal artery to the occlusion in case of dilated high-capacitance collaterals.

Table 1 Diagnostic criteria for PAD using Doppler examination

	Diameter reduction	Waveform	Spectral broadening	PSV distal/proximal
Normal	0	Triphasic	Absent	+++ No change
Mild	1%-19%	Triphasic	Present	<2:1
Moderate	20%-49%	Biphasic	Present	<2:1
Severe	50%-99%	Monophasic	Present	>2:1*

* > 4:1 suggests > 75% stenosis, > 7:1 suggests > 90% stenosis

Furthermore, patients' Doppler data were quantitatively evaluated as physiological signals, fine monophasic signals, weak monophasic signals or weak monophasic signals combined with a diastolic forward flow[63, 64]. ACCmax and RPSI were compared between these four waveform sub-groups. The principle used to differentiate weak monophasic signals from fine weak monophasic signals was a peak velocity lower than 30cm/s, and the principle used to characterise weak monophasic signals combined with a diastolic forward flow is plotted in **Figure 4**.

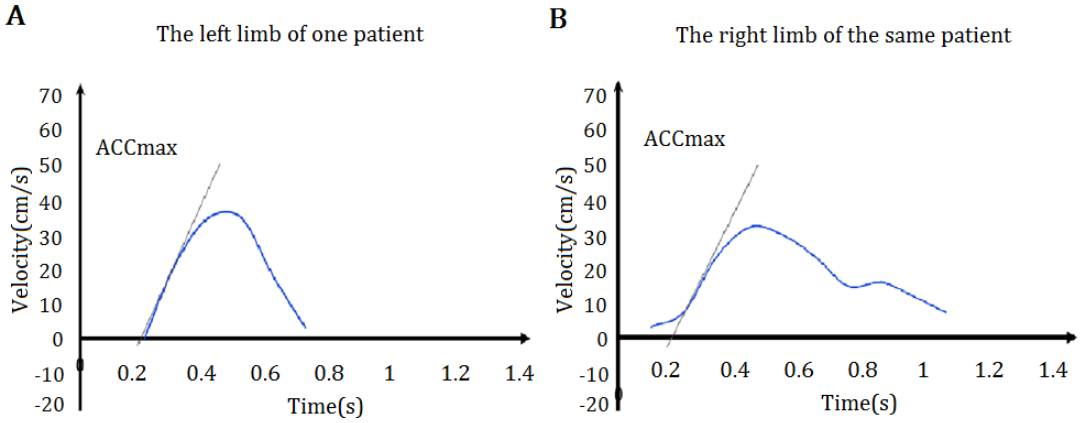

Figure 4 Two types of weak monophasic waveforms due to different stages of limb ischemia. Figure 4A is weak monophasic with a peak velocity of about 30 cm/s; Figure 4B is characterised by a peak velocity of 30 cm/s as well as a continuous forward flow wave, which is absent in Figure 4A.

For newly referred patients who had indications of revascularisation, angiography of each segment of the lower-limb arteries was employed. Since the accuracy of the visual assessment of intervention has been disputed by physicians[65], a standardised quantitative analysis method was used instead of a visual angiogram (Sanders Data Systems, USA), and the major lesion was calculated automatically and recorded as a percentage of stenosis[60]. **Figure 5** shows an example of a quantitative analysis of stenosis in PAD cases.

Based on the quantitative grades of stenosis, the overall pathological locations and severity were accumulated according to the Bowling scoring system[66]: PAD was confirmed with any segment of haemodynamic related stenosis (> 50% diameter reduction); stenosis was further semi-quantitatively scored as 0 < 50%, 1 < 75% and 2 > 75% of obstructive lesions. When there were multiple stenosis in one limb, the highest score was used in the analysis.

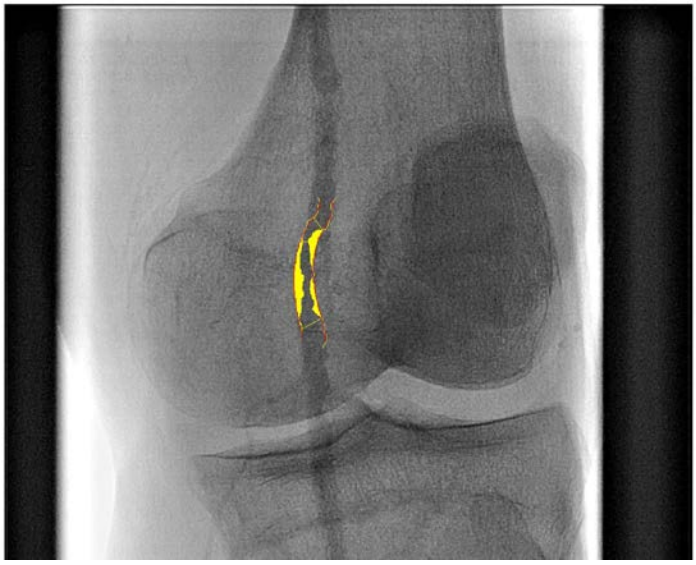

Figure 5 Quantitative vascular analysis produced during the procedure using Sanders Data Systems (USA). The red lines are the reconstructed reference contours and are marked in the image along the vascular wall, while the yellow area represents the stenosis lesion in this selected angiographic view. The actual obstruction diameter was 1.17 mm, and the referred diameter of the narrowing lesion was 3.46 mm, yielding a percentage diameter stenosis of 66%.

3.6 Endovascular procedure and post-intervention surveillance

For 25 newly suspicious PAD patents who suffered from severe or high-grade lesions, ultrasound-derived ACCmax and RPSI assessments were conducted one day before angiography as baseline parameters and one day thereafter as surveillance variables. The revascularisation procedures have been reviewed elsewhere[59]. Traditional post-intervention surveillance is conducted using a duplex ultrasound at the recurrence of ischemic symptoms, or performed once a year after the revascularization. The pulsed wave Doppler and colour Doppler could characterise the revascularized vessels. In the current study, the aim was to estimate the severity

of the distant perfusion deficit before revascularisation and the haemodynamic improvement after revascularisation using the values of ACCmax and RPSI[67].

3.7 Practice of modulating ACCmax and RPSI-derived FSS under ECP pressure

The 18 healthy volunteers underwent one session of standard ECP treatment. The ultrasound-derived ACCmax and RPSI evaluations were measured on carotis. The pressure of the ECP device increased every 5 minutes in the sequence of 40 mmHg, 80 mmHg, 120 mmHg, 160 mmHg and 200 mmHg. The various haemodynamic parameters were collected from each volunteer, as illustrated by **Table 2**.

Table 2 Pressure values during the examination of flow

	0mmHg	40 mmHg	80 mmHg	120mmHg	160 mmHg	200 mmHg	0mmHg
Vmean	x	x	x	x	x	x	x
Systolic ACCmax	x	x	x	x	x	x	x
Systolic RPSI	x	x	x	x	x	x	x
Diastolic ACCmax	x	x	x	x	x	x	x
Diastolic RPSI	x	x	x	x	x	x	x

3.8 Statistics

The number of required samples was statistically estimated before the clinical study to obtain the statistical power of 80%. The numerical data were first tested for normal distribution by Kolmogorov-Smirnov tests. When the data were non-normally distributed, the descriptive statistics for quantitative measures were median and quartiles (25th and 75th percentiles). The categories were described as absolute and relative (%) frequencies. The groups defined by PAD status were compared using the Wilcoxon rank sum test or Fisher's exact test, as appropriate. To determine the diagnostic properties, the haemodynamic measures were evaluated using the ROC analysis. The AUC and optimal threshold were set as defined by the Youden criterion, which maximises the distance to the diagonal identity. Additional thresholds were determined for sensitivity or specificity of 90%. For these thresholds, sensitivity, specificity, PPV and NPV were reported. The relations between measures were explored graphically by a linear regression, non-linear regression (local polynomial regression fitting LOESS) and quadratic regression. Quadratic regression models were computed with an R^2 value. Two approaches were explored to combine different diagnostic methods. The first approach involved using the logistic regression as a linear model, which utilised the complete data set of each individual. Based on the predicted probabilities for PAD, subjects with a probability > 50% were classified as test-positive, and the diagnostic properties were calculated accordingly. The second approach involved a parallel test,

which was used to identify a subset as a screen test positive with any positive result from ACCmax, RPSI or ABI. The statistical analysis was performed using R language, and the tests were considered to be significant if the two-side P value was < 0.05.

4 Results

4.1 Diagnosis of PAD

4.1.1 Demographic variables

There were 91 non-diabetic participants and 77 diabetic participants. Among the 168 participants, all haemodynamic parameters of each available infrapopliteal artery were recorded. The baseline characteristics of all 168 participants (arteries, n = 310) are presented in **Table 3**.

Furthermore, demographic variables were collected, including incidence of blood hypertension (systolic Bp > 140 mmHg, diastolic Bp > 90 mmHg or both; or under control using of Bp-lowering therapy), diabetes (self-documented presence of high levels of blood sugar, or use of anti-diabetic medicine or insulins), dyslipidaemia (self-documented presence of dyslipidaemia, or use of anti-dyslipidaemia medicines), coronary vascular disease (CVD) (documented history of myocardial infarction, acute coronary syndrome, percutaneous coronary intervention or coronary artery bypass graft) and chronic kidney disease (CKD) (defined as a moderate reduction in the glomerular filtration rate (30–59 ml/min/1.73 m^2)).

In each diabetic and non-diabetic group, about 50% of patients suffered from PAD. Similarly, there was no distinction in the distribution of patients suffering from CAD, CKD and ABI within the diabetic or non-diabetic groups; however, **Table 3** shows that more HBP (blood hypertension) patients were included in the non-diabetic group.

Table 3 Baseline characteristics of all study participants, including non-diabetic and diabetic populations

	Non-Diabetic Population (n = 150)*	Diabetic Population (n = 160)*	P-value
Age	69 ± 8	69 ± 10	0.397
Gender (F/M)	56/94	46/114	0.15
CVD (no/yes)	39/111	27/133	0.05
CKD (no/yes)	100/35	108/39	0.91
HBP (no/yes)	36/114	20/140	0.009
PAD (no/yes)	73/77	84/76	0.50
ABI	0.97 ± 0.32	1.04 ± 0.38	0.06
ATA/ATP	87/63	80/80	0.52

* Sample size n refers to the number of arteries.

4.1.2 Technical applicability

The waveforms of varying pathological appearances were displayed quantitatively, and the values are given in **Figure 6A-D**. **Figure 6A** shows an example of the flow measurement on the

tibial arteries of PAD in unaffected patients using a Doppler-derived device. **Figure 6B-D** shows examples of Doppler-device measurements on the tibial arteries of PAD-affected patients. The waveform patterns exhibited different signals, such as fine monophasic signals, weak monophasic signals and weak monophasic signals complicated by a diastolic forward flow (**Figure 6B-D**). Different velocity profiles under ultrasound beams were then sampled by applying the spectrum analysis algorithm using MATLAB (layout II of **Figure 6A-D**). On the digitalised flow velocity profile, the X-axis represents the time (in seconds), and the Y-axis represents the velocity of the blood flow (in mm^2/s). The averages of the velocity curves are indicated by the green lines (layout III of **Figure 6A-D)**. The mean velocity from one cardiac cycle and the corresponding maximal acceleration were assessed to calculate RPSI. The statistical test showed that the measurement error was lower than 5% (data not shown). Combining the qualitative and quantitative validation, the real-time spectrum analysis was robust for the transformation and measurement of varying Doppler signals of tibial arteries.

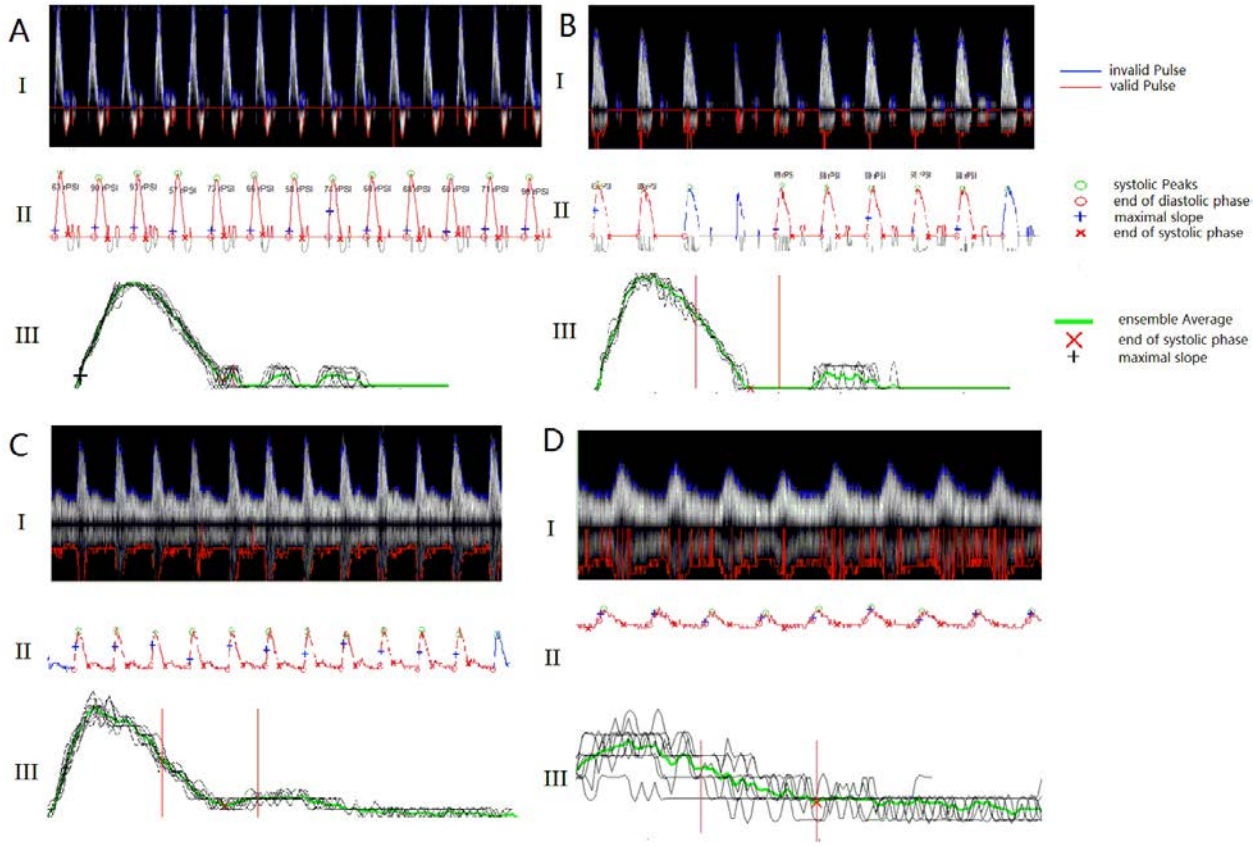

Figure 6 Examples showing the procedure of the Gefäßtachometer programme. A. Triphasic waveform. B. Fine monophasic signals. C. Weak monophasic signals. D. Weak monophasic signals complicated by a diastolic forward flow. I. Waveform captured within 15 seconds under pulse-waved mode. II. Computational contoured curves during the systolic phase. III. Ensemble of velocity-time curve using the average method. The black cross represents the dot with maximal acceleration. On each figure, the X-axis represents the time (in seconds), and the Y-axis represents the velocity values of blood flow (in cm/s).

4.1.3 Haemodynamic characteristics

The Doppler-derived ACCmax and RPSI data measured in PAD and non-PAD patients are shown in **Figure 7**. In line with the method of ABI calculation, the ratio of ACCmax on legs and arms was also analysed and defined as the ACCmax-ratio. Due to non-normal distribution, median and quantiles were calculated: ACCmax-ratio values were 790 (589/1056) cm/s^2 and 396 (262/564) cm/s^2, RPSI-ratio values were 98 (75/130) s^{-1} and 53 (24/97) s^{-1}, and ACCmax-ratio values were 1.03 (0.75/1.47) and 0.62 (0.36/1.19) in PAD and non-PAD, respectively. After applying the Wilcoxon rank sum test, all values showed statistical differences between the PAD and non-PAD groups ($P < 0.005$).

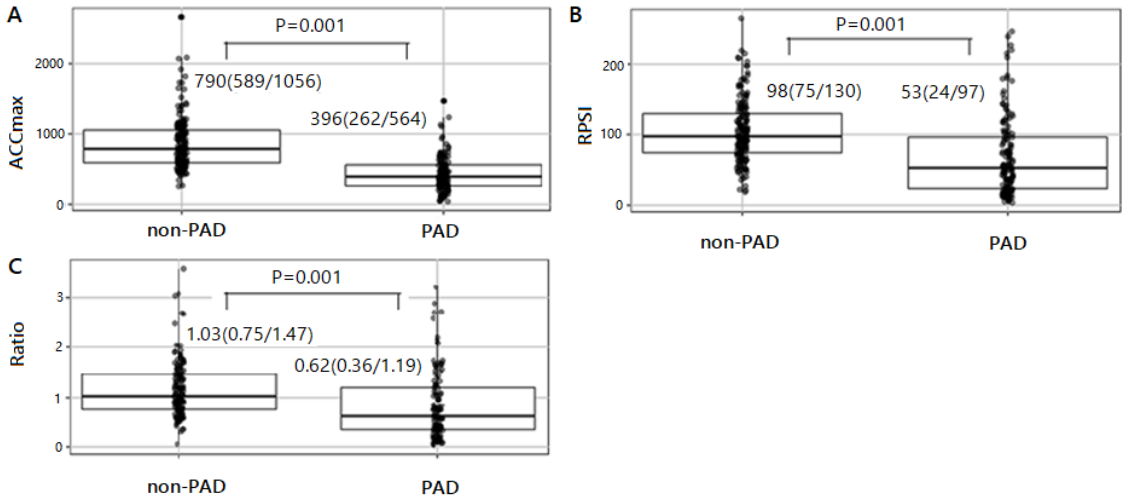

Figure 7 Comparison between the non-PAD group and PAD group in terms of ACCmax values, RPSI values and ACCmax-Ratio values. ACCmax: systolic maximal acceleration; RPSI: relative pulse slope index. A. ACCmax in non-PAD and PAD groups were 944.58 ± 373.42 cm/s^2 and 421.16 ± 194.62 cm/s^2 ($p = 0.000 < 0.005$), respectively. B. RPSI in non-PAD and PAD groups were 105.67 ± 49.68 s^{-1} and 64.27 ± 46.38 s^{-1} ($p = 0.000 < 0.005$), respectively. C. ACCmax-ratio in non-PAD and PAD groups were 1.03 ± 0.25 and 0.62 ± 0.39 ($p > 0.05$), respectively.
*Similar to the ABI calculation, the ACCmax-ratio was defined as the quotient of ACCmax on the leg and arm.

To compare the haemodynamic characteristics between different stages of PAD, the waveform characteristics and flow velocity were taken into account. Samples were sub-grouped as physiological signals, fine monophasic signals, weak monophasic signals and weak monophasic signals complicated by a diastolic forward flow (n = 152, 58, 64, 35). In each sub-group of physiological signals, fine monophasic signals, weak monophasic signals and weak monophasic signals complicated by a diastolic forward flow, the ACCmax values were 924 ± 370 cm/s^2, 505 ± 169 cm/s^2, 459 ± 132 cm/s^2 and 191 ± 119 cm/s^2, respectively, and the RPSI values were 105 ± 43 s^{-1}, 57 ± 33 s^{-1}, 116 ± 55 s^{-1} and 19 ± 15 s^{-1}, respectively **(Figure 8)**. It was observed that ACCmax was similar between the fine monophasic sub-group and the weak monophasic sub-group, but RPSI showed a significant difference between them ($P< 0.01$).

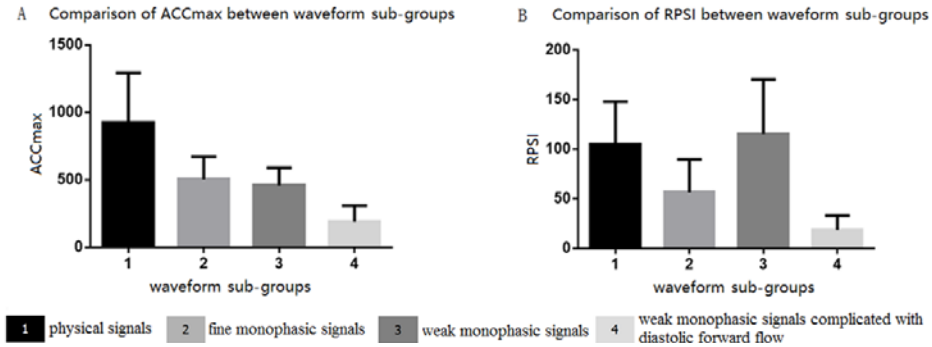

Figure 8 Comparison of haemodynamic values between different waveform sub-groups. A. Comparison of ACCmax values between different waveform sub-groups. B. Comparison of RPSI values between different waveform sub-groups.

To determine whether the new parameters and ABI were comparable, the association between ACCmax and ABI as well as the association between RPSI and ABI were assessed using a regression analysis (**Figure 9A, Figure 9B**). Linear, quadratic and logarithmic analyses were conducted, and the strongest association was established by a quadratic relationship. The adjusted coefficient of determination (R^2) was 0.131 for the association between ACCmax and ABI, and R^2 was 0.083 for the association between RPSI and ABI. **Figure 9A** demonstrates the pair of ACCmax and ABI in all samples, non-diabetic samples and diabetic samples, respectively; **Figure 9B** shows the pair of RPSI and ABI in all samples, non-diabetic samples and diabetic samples, respectively. The red points represent non-PAD, and the blue points represent PAD. The quantitative analysis of the diagnostic performance of ABI and ACCmax showed that false negative ABI values were observed in the range of ABI of 0.9–1.3 as well as ≥ 1.30, while ACCmax values were unequivocally lower in the PAD samples than in non-PAD samples.

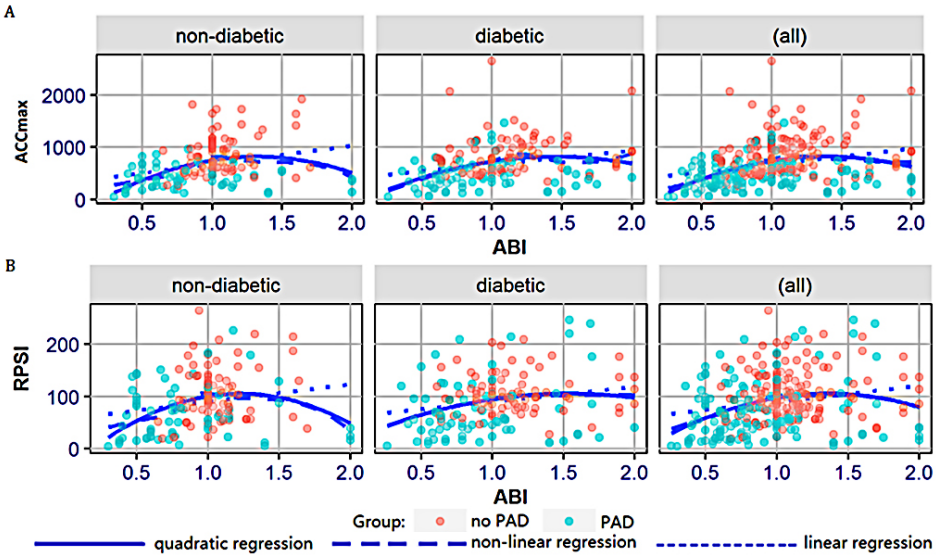

Figure 9 The correlation between novel parameters and ABI values. A. Association analysis between ACCmax and ABI. Quadratic regression was computed with adjusted R^2 = 0.131 ($P < 0.01$). B. The association analysis between RPSI and ABI; quadratic regression with adjusted R^2 = 0.083.

During the evaluation of the angiography results, the degree of stenosis from the iliac artery to the tibial artery was semi-quantitatively measured. When there were multiple stenosis in one artery, the most severe was chosen, and then the percentage of stenosis was calculated. The associations between the percentage of stenosis and the new parameters of the ACCmax, RPSI and ACCmax-ratio (in each **Figure 10A, 10B and 10C)** were analysed. They showed that the ACCmax values decreased steadily in inverse proportion with the increasing stenosis degree. Likewise, the RPSI values and ACCmax-ratio values showed lower values when stenosis was exacerbated. The association coefficient of ACCmax was more significant than that of RPSI and ACCmax-ratio.

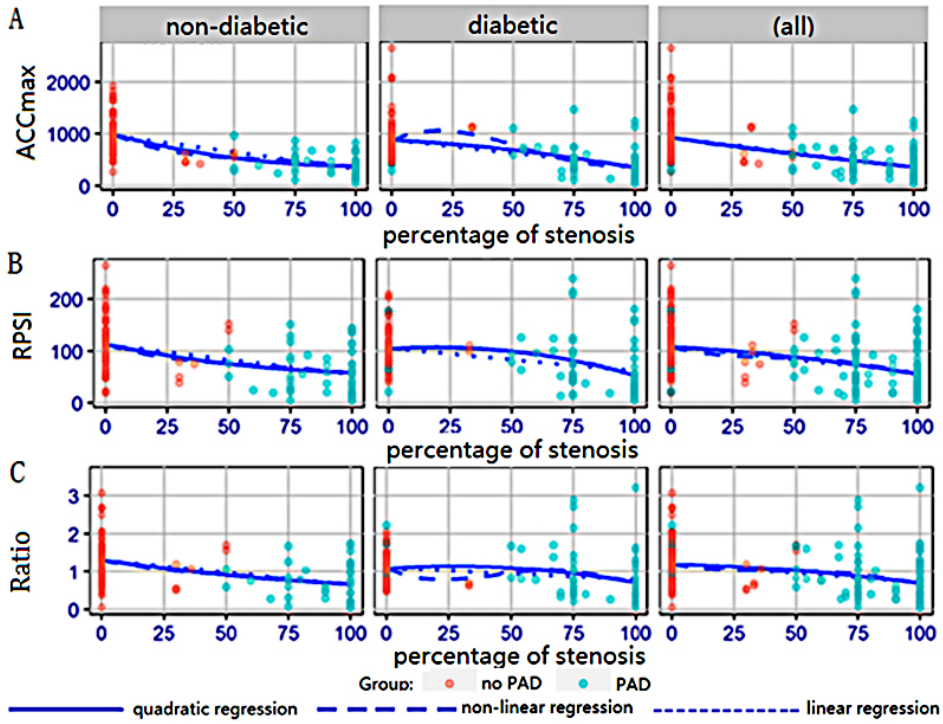

Figure 10 The correlation between novel parameters and stenosis percentage. A. Correlation between ACCmax values and degree of stenosis using a quantitative evaluation adjusted $R^2 = 0.36$ ($P < 0.001$). B. Correlation between RPSI values and degree of stenosis using a quantitative evaluation adjusted $R^2 = 0.173$ ($P < 0.001$). C. Correlation between ACCmax-ratio values and degree of stenosis using a quantitative evaluation adjusted $R^2 = 0.116$ ($P < 0.001$).

4.1.4 Diagnostic cut-off values in non-diabetic and diabetic populations, respectively

To validate the diagnostic thresholds in non-diabetic populations, 131 artery properties from 80 non-diabetic participants were analysed. Fifty-seven records were from non-PAD participants, and 74 were from PAD participants. Angiography was used as the gold standard. In general, the diagnostic reliability of ACCmax was higher compared with that of RPSI. The results showed that the area under the curves (AUC) of ACCmax and RPSI were 0.88 and 0.73, respectively, in the non-diabetic population (**Figure 11A)**. Furthermore, the AUC of ABI and ACCmax-ratio

were 0.75 and 0.72, respectively. The optimal ACCmax cut-off of 503 cm/s^2 had a sensitivity of 74%, a specificity of 88%, accuracy of 82%, an NPV of 81% and a PPV of 83%. The optimal RPSI cut-off of 58 s^{-1} had a sensitivity of 46%, a specificity of 93%, accuracy of 72%, an NPV of 68% and a PPV of 83%.

As a screening test, the ACCmax, RPSI and ACCmax-ratio were observed to better predict PAD- affected participants. A threshold with a sensitivity of 90% was observed (**Figure 11B, Figure 11C and Figure 11D)**. The ACCmax threshold with a sensitivity of 90% was 693 cm/s^2 (specificity of 60%, accuracy of 74%, NPV of 89% and PPV of 65%). In addition, thresholds with a specificity of 90% were also calculated to better exclude PAD-unaffected participants. The ACCmax threshold with a specificity of 90% was 476 cm/s^2 (sensitivity of 68%, accuracy of 80%, NPV of 78% and PPV of 85%). The extra thresholds of RPSI and of ACCmax-ratio failed to demonstrate the diagnostic performance of ACCmax.

A

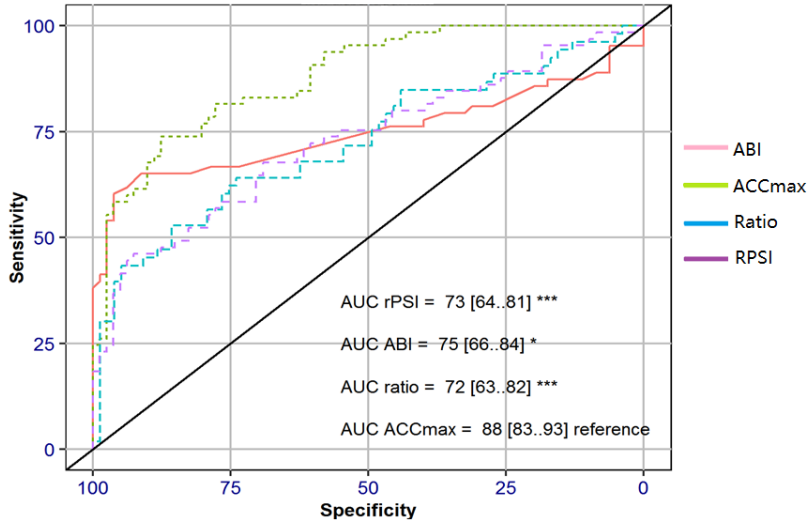

B

ACCmax	ROC_AUC	Threshold	Specificity	Sensitivity	Accuracy	NPV	PPV
Accuracy	88 [83..93]	498	88	74	82	81	83
90% Sensitivity		693	60	91	74	89	65
90%Specificity		476	90	68	80	78	85

C

RPSI	ROC_AUC	Threshold	Specificity	Sensitivity	Accuracy	NPV	PPV	P value
Accuracy	73 [64..81]	45	93	46	72	68	83	0.001
90% Sensitivity		142	18.5	91	51	71	47	
90%Specificity		49	90	46	71	68	79	

D

Ratio	ROC_AUC	Threshold	Specificity	Sensitivity	Accuracy	NPV	PPV	p V.S.. ACCmax
Accuracy	72 [63..82]	0.63	86	53	72	73	72	0.001
90% Sen		1.66	18.2	91	48	74	43	
90%Spe		0.54	91	45	72	71	77	

Figure 11 The diagnostic performance of new parameters in non-diabetic populations. A. ROC curve of RPSI, ACCmax, ACCmax-ratio and ABI. B. Cut-off values of ACCmax. C. Cut-off values of RPSI, and the P value against the performance of ACCmax is < 0.05. D. Cut-off values of ACCmax-ratio, and the P value against the performance of ACCmax is < 0.05.

In diabetic populations, 160 artery properties were analysed. Among them, 84 records were non-PAD, and 76 were PAD. The AUC was 0.85 and 0.74 with ACCmax and RPSI measurements, respectively, based on the ROC analysis (**Figure 12A**). The performances of ABI and ACCmax-ratio had an AUC of 0.70 and 0.67, respectively. In the diabetic population, the optimal threshold of ACCmax was calculated to be 444 cm/s^2, with a PPV of 96% and an NPV of 72%. The optimal threshold of RPSI was calculated to be 74 s^{-1} in the diabetic population, with a PPV of 91% and an NPV of 71%.

For the diabetic populations, the thresholds of ACCmax, RPSI and ACCmax-ratio were also calculated with a sensitivity of 90% (**Figure 12**B, **Figure 12**C and **Figure 12**D**)**. The ACCmax threshold with a sensitivity of 90% was 745 cm/s^2 (specificity of 58%, accuracy of 73%, NPV of 87% and PPV of 66%). The thresholds with a specificity of 90% were also calculated to better exclude PAD-unaffected participants. The ACCmax threshold with a specificity of 90% was 489 cm/s^2 (sensitivity of 61%, accuracy of 77%, NPV of 72% and PPV of 85%). The extra thresholds of RPSI and the ACCmax ratio failed to demonstrate the diagnostic performance of ACCmax.

A

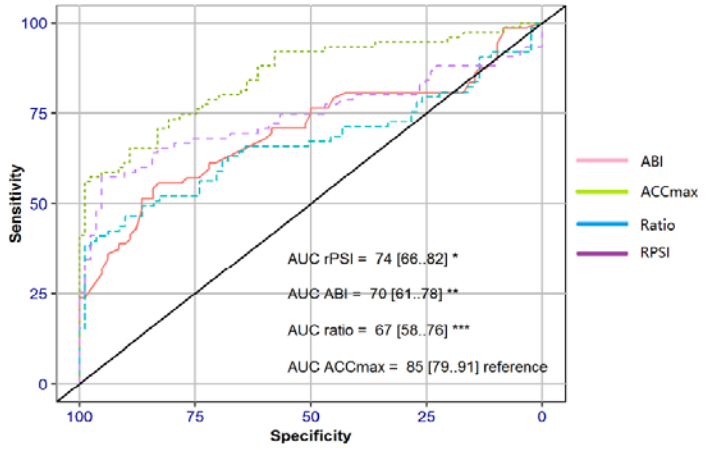

B

ACCmax	ROC_AUC	Threshold	Specificity	Sensitivity	Accuracy	NPV	PPV
Accuracy	85 [79..91]	444	98	57	78	72	96
90% Sensitivity		745	58	91	73	87	66
90%Specificity		489	90	61	77	72	85

C

RPSI	ROC_AUC	Threshold	Specificity	Sensitivity	Accuracy	NPV	PPV	P value
Accuracy	74 [66..82]	58	95	57	77	71	91	0.014
90% Sensitivity		165	9.6	91	48	53	48	
90%Specificity		63	90	59	75	71	85	

D

Ratio	ROC_AUC	Threshold	Specificity	Sensitivity	Accuracy	NPV	PPV	pV.S.. ACCmax
Accuracy	67 [58..76]	1	96	41	70	64	91	0.001
90% Sen		2	14	90	50	61	49	
90%Spe		1	90	47	69	65	81	

Figure 12 The diagnostic performance of new parameters in diabetic populations. A. ROC analysis of ACCmax and RPSI in the diabetic population. B. Cut-off values of ACCmax. C. Cut-off values of RPSI, and the P value against the performance of ACCmax is < 0.05. D. Cut-off values of ACCmax-ratio, and the P value against the performance of ACCmax is < 0.05.

4.1.5 Diagnostic strategy with combination models

Based on the information regarding the respective diagnostic performances of ACCmax, RPSI, ACCmax-ratio and ABI, we further investigated whether a more accurate prediction would be obtained by combining the indices. The multi-variable deviance test showed that the significance level of ACCmax was less than 0.001, and that of ABI was less than 0.01 (**Figure 13B**). Using the logistic regression model, the probability value of the presence of PAD was calculated for each subject. Subsequently, the ROC analysis was applied to evaluate the diagnostic performance of the newly calculated possibility values (**Figure 13A**). The optimal threshold of probability values was 0.52 using the maximal Youden Index, and the additional threshold was computed as 0.32 with 90% of sensitivity and 0.61 with 90% of specificity (**Figure 13C**). The comparison between the logistic regression model and the single ACCmax method showed a similar level of AUC.

A

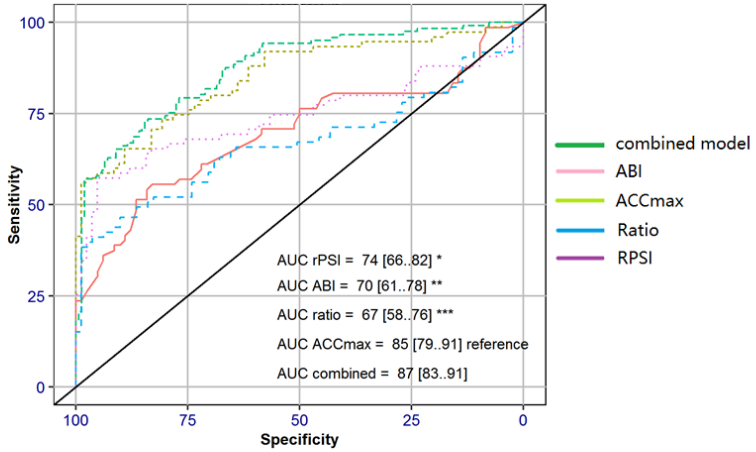

B

	LR Chisq	Df	
RPSI	0.099	1	0.75266
ACCmax	80.962	1	< 2e-16 ***
ratio	0.368	1	0.54391
ABI	9.200	1	0.00242 **

C

Cut-Off	ROC_AUC	Threshold	Specificity	Sensitivity	Accuracy	NPV	PPV	P
Accuracy	87 [83..91]	0.52	84	74	79	80	78	0.559
90% Sensitivity		0.32	62	90	74	89	65	
90% Specificity		0.61	90	65	79	77	84	

Figure 13 A. ROC curve obtained from diabetic patients' data; AUC of combining approach is 87%. B. Analysis of Deviance Table (Type II tests). Significant level was marked with ** or ***. C. The cut-off values of the compositional prediction against the performance of ACCmax are < 0.05.

Next, whether or not the diagnostic performance could be improved using the parallel test method was investigated. In this analysis, the diagnostic standard for PAD was either the positive value of ACCmax or the positive value of RPSI. The cut-off values of ACCmax and RPSI were < 503 cm/s^2 and < 58 s^{-1}, respectively, based on the results of the single parameter evaluation. The threshold of ABI was < 0.9. The parallel process is shown in **Figure 14**. In non-

PAD patients (panels A and B), false positive results were < 10% for either the parallel test or ABI measures. Comparing panel C with panel D, more false positives were observed with the ABI measures (blue points) in diabetics (panel D) than in non-diabetics (panel C). The parallel test detected a large number of missing points with ABI measures (blue points inside the yellow and green areas).

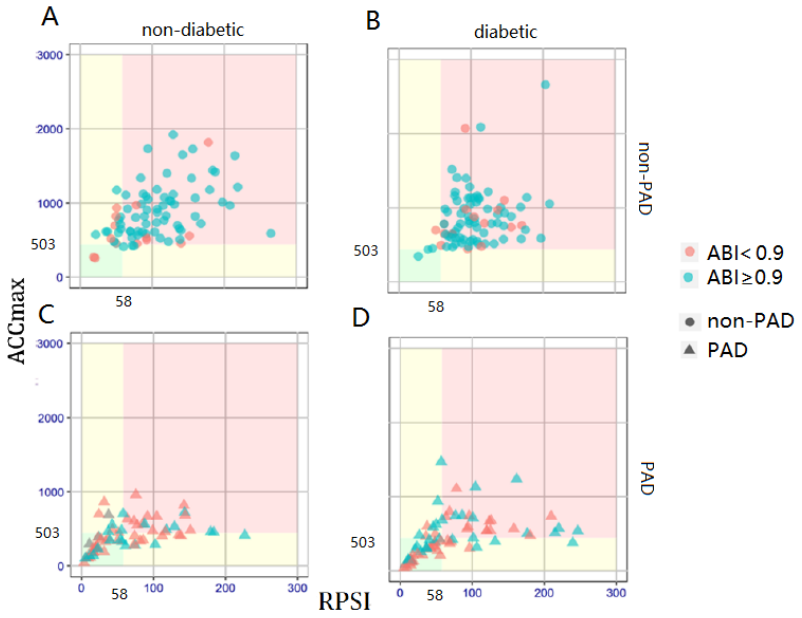

Figure 14 Parallel test using measures of ACCmax and RPSI. In each panel, the threshold of ACCmax was shown as < 503 cm/s^2 and as < 58 s^{-1} for RPSI. Thus, the green zone shows the double positive values of ACCmax and RPSI; the pink zone shows individuals with double negative parameters. The yellow zone shows individuals with single positive parameters.

The diagnostic efficiency of the parallel test and the ABI method was calculated and compared in both the non-diabetic and diabetic groups (**Figure 15**). Consistent with the scatter distribution in **Figure 14**, the parallel test achieved a considerable level of specificity (95%) in diabetic populations, which was much higher than the ABI method. The sensitivity of the parallel test was also higher than the ABI method both in diabetic and non-diabetic populations.

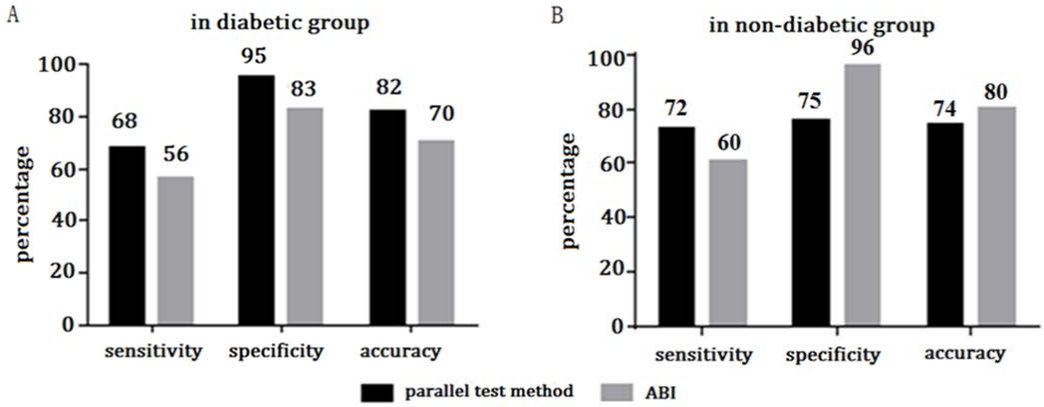

Figure 15 Comparison of diagnostic sensitivity, specificity and accuracy in diabetic and non-diabetic groups.

The two combinational models revealed that the shortcoming of the logistic regression was the absence of recursion and that the models could compensate for the imperfections of the parallel test. Therefore, a more complex approach of a regression tree (one data mining technique) was investigated, which defined a set of rules instead of relying on predefined thresholds. Thus, splits can be made based on surrogates. Furthermore, no assumptions were made regarding the linearity of the relation between diagnostic measures and the risk of PAD. In this analysis, cross-validation based on a jack-knife procedure was applied. Each patient was classified based on a regression tree build on all members of the study. Similar leave-one-out classifications were done for all other tests of diagnostic properties, as the same circular problem applies (**Figure 16**). The diagnostic sensitivity and specificity increased simultaneously. In diabetic participants, the sensitivity increased to 88%, and the specificity increased to 84%.

A

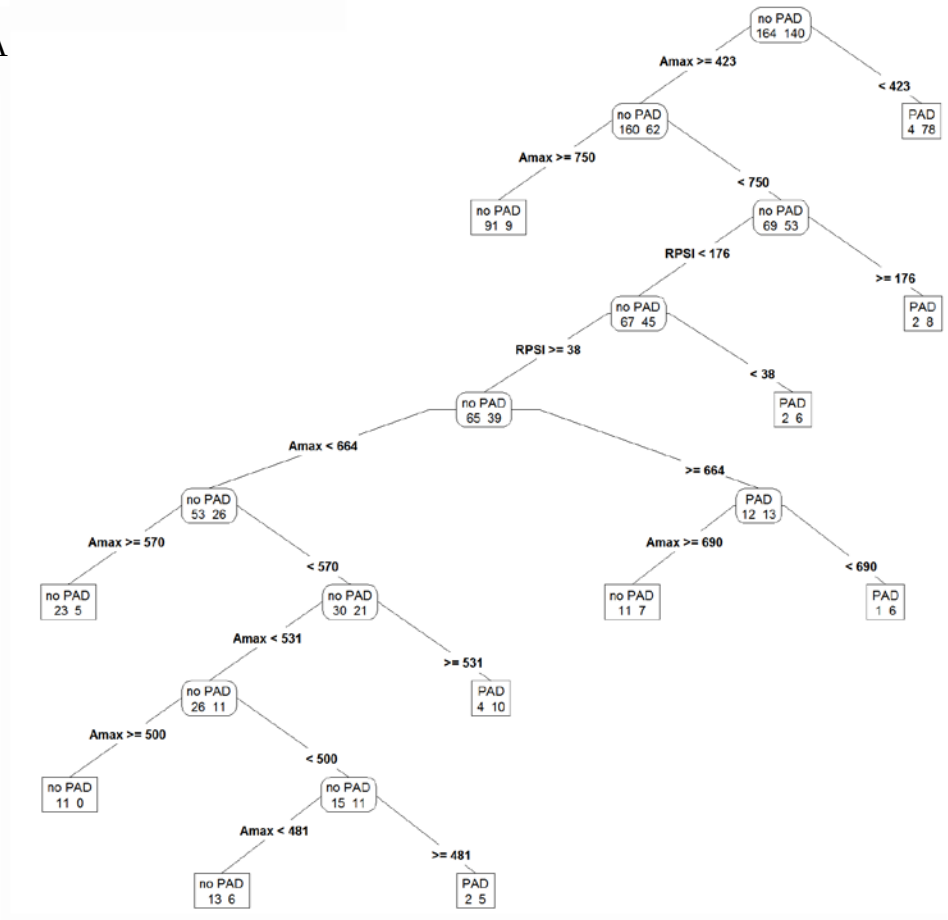

B

Group	Sensitivity	Specificity	Accuracy
All patients	81	91	86
Non-diabetic patients	82	86	84
Diabetic patients	88	84	86

Figure 16 The combination model of a decision tree. A. An exploratory example of a decision tree in diabetic participants. B. Diagnostic properties using a decision tree. The sensitivity of all participants was 81%, but it was improved in particular diabetic participants to 88%.

4.2 Post-revascularisation surveillance

In the second part of this work, 25 PAD patients who were subjected to an invasive revascularisation procedure were enrolled. Therefore, ACCmax and RPSI were measured on 44 distal tibial arteries. Individual comparisons were conducted using measurements one day before intervention and one day after intervention. The changes in the haemodynamic variables of ACCmax, RPSI and ACCmax-ratio are shown in **Table 4**. It is apparent that the ACCmax values increased, whereas the RPSI values decreased after revascularisation. Both of these alterations had significant differences before and after revascularisation.

Table 4 Haemodynamic variables before and after revascularisation.

* ACCmax-ratio was calculated as ACCmax (leg)/ACCmax (brachialis).

	Before	After	Difference	P value
ACCmax(leg) (cm/s^2)	427.83 ± 171.67	509.30 ± 171.23	81.48 ± 159.50	0.002
RPSI(leg) (s^{-1})	82.17 ± 58.76	64.08 ± 39.65	-18.09 ± 50.56	0.022
Vmean(leg) (cm/s)	7.04 ± 3.80	9.63 ± 4.09	2.58 ± 4.17	0.003
ACCmax-ratio	0.61 ± 0.31	0.65 ± 0.50		0.442

Moreover, in order to evaluate the correlation between improvement of haemodynamic values (dACCmax and dRPSI) and their baseline levels, regression analysis was computed between dACCmax and baseline ACCmax, dRPSI and baseline RPSI respectively. A strong correlation between dACCmax and the base level of ACCmax was observed, as well as the correlation between dRPSI and the base level of RPSI (**Figure 17A, Figure 17B**). As shown in decreasing tendency in both figures, the moderate level of baseline ACCmax or RPSI was correlated with the moderate improvement of ACCmax or RPSI; the low level of baseline ACCmax or RPSI was correlated with a high level of improvement of ACCmax or RPSI.

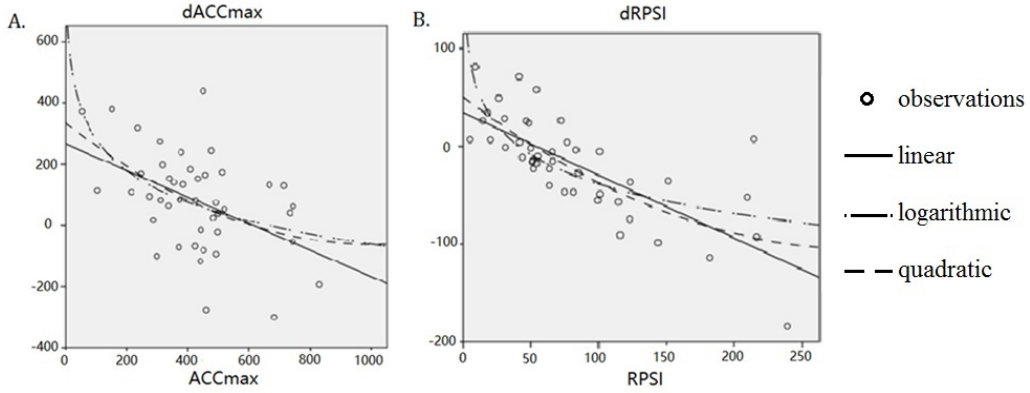

Figure 17 The correlation between base levels of ACCmax and RPSI and the improvement of ACCmax and RPSI. dACCmax: ACCmax before revascularisation subtracted from ACCmax thereafter; dRPSI: RPSI before revascularisation subtracted from RPSI thereafter. A. The correlation between the improvement of ACCmax (dACCmax) and the base level of ACCmax (Pearson coefficient: -0.467, 0.01 level). B. The correlation between the improvement of RPSI (dRPSI) and the base level of RPSI (Pearson coefficient: -0.747, 0.01 level).

In addition, differences of hemodynamic flow parameters were measured in the anterior tibial artery (ATA) and the posterior tibial arterial (ATP) from each lower limb. (Note: in some patients, only one artery were examined because of an acute or chronic occlusion of the second tibial artery). Considering the change of Vmean, ACCmax and RPSI before and after revascularization, the in-pair t-test showed no difference between the haemodynamic indices of dVmean, dACCmax, dRPSI from ATP and from ATA of the same leg (**Table 5**).

Table 5 Comparison of changes in the haemodynamic indices from the ATP and ATA of the same leg

	ATA	ATP
dVmean	2.70 ± 3.94	3.59 ± 3.94
dACCmax	55.82 ± 182.21	104.59 ± 134.02
dRPSI	-28.41 ± 61.40	-14.91 ± 42.75

4.3 The real-time dynamics of ACCmax and RPSI under ECP

In the third part of the study, the dynamic changes of ACCmax and RPSI values of carotis under ECP treatment within 18 healthy volunteers were observed, in order to investigate the reaction of ACCmax and RPSI under acute flow changes. Considering the pro-arteriogenic effect and FSS-enhancing mechanism of ECP, we aimed to explore the optimal ECP pressure for increasing the flow to archive the highest FSS values. Therefore, ACCmax and RPSI changes were investigated. Even though the correlations between various haemodynamic values and ECP pressure were not observed generally (shown in **Table 6**), haemodynamic values reacted to ECP pressure individually different, and some individuals showed obvious change of haemodynamic values along with the increasing of ECP pressure (shown in **Figure 18**).

Table 6 Haemodynamic parameters under one session of ECP. A. The treatments were done in a succession of 0 mmHg, 40 mmHg, 80 mmHg, 160 mmHg and 200 mmHg, and these measures were observed: Vmean, systolic ACCmax, systolic RPSI, diastolic ACCmax and diastolic RPSI.

Carotis	0 mmHg	40 mmHg	80 mmHg	120 mmHg	160 mmHg	200 mmHg
Vmean	30.1 ± 4.11	30.03 ± 4.37	30.68 ± 4.87	29.53 ± 4.08	29.87 ± 5.22	31.12 ± 4.36
$SysA_{max}$	1199.5 ± 141.8	1199.5 ± 129.9	1257.1 ± 218.8	1216.7 ± 185.4	1286.4 ± 195.0	1271.7 ± 217.7
Sys RPSI	41.78 ± 8.27	42.19 ± 7.97	43.00 ± 7.76	44.76 ± 10.09	45.97 ± 8.71	44.84 ± 11.70
Dias A_{max}	256.13 ± 93.4	243.86 ± 68.9	236.30 ± 87.3	265.70 ± 92.7	278.88 ± 101.2	271.95 ± 105.7
Dias RPSI	9.13 ± 4.49	8.47 ± 2.38	7.81 ± 2.37	9.19 ± 2.25	9.64 ± 2.71	9.11 ± 3.31

Taking the increasing diastolic pressure under ECP treatment into account, the diastolic ACCmax changes in response to different ECP treatment pressures were investigated in more detail. As shown in **Figure 18**, the divergent change tendencies of diastolic ACCmax values under ECP pressure were observed in each individual. Among them, it was observed that the maximal amplitude of diastolic ACCmax increased approximately 200%, which is shown in pi01,

pi03, pi05, pi07, pi14, pi18, pi21, pi22 and pi23 of **Figure 18**.

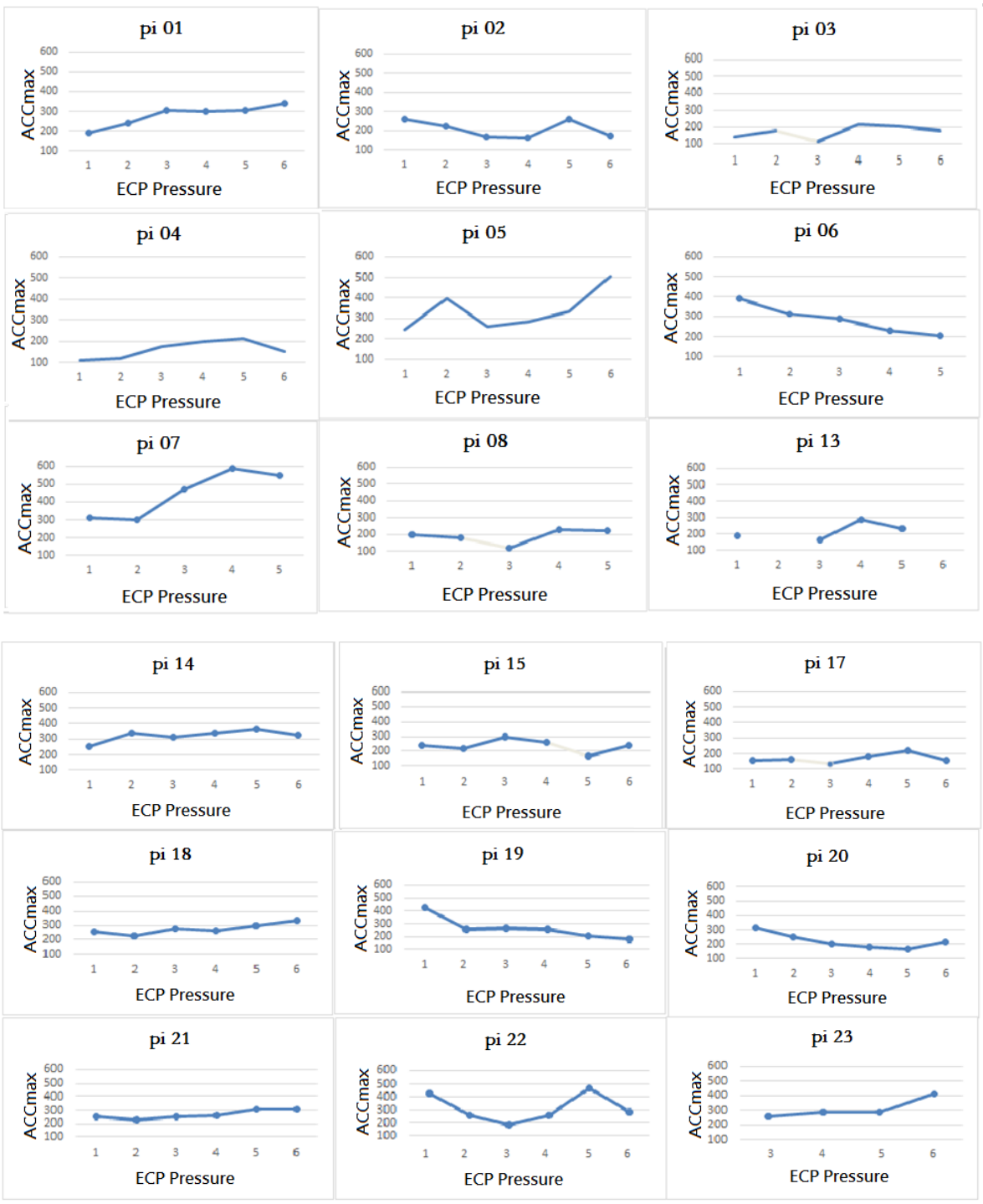

Figure 18 Scatter-plot of diastolic ACCmax values from each participant under the sequence of ECP pressures (pi01–pi23). The X-axis represents the pressure of the ECP machine in which 1, 2, 3, 4, 5 and 6 represent 0 mmHg, 40 mmHg, 80 mmHg, 120 mmHg, 160 mmHg and 200 mmHg, respectively. The Y-axis represents the diastolic ACCmax values with a dimension of cm/s^2.

5 Discussion

In the last 20 years, complex reconstruction techniques (e.g. 3D Doppler) have provided numerous advancements for the quantitative analysis of blood flow; however, the simpler 1D analysis models, such as Doppler measurements, have recently been used because they can simplify conditions for a more global patient-specific context[68]. In this study, a comprehensive screening of ACCmax and RPSI as novel diagnostic parameters for use in the 1D analysis of PAD was performed.

First, this work presents a clinical study in which the novel diagnostic parameters ACCmax and RPSI were evaluated in 168 patients to diagnose PAD in a diabetic population. The calculations showed that the optimal threshold for ACCmax to detect PAD was 444 cm/s^2. The positive predictive value (PPV) was 96%, and the negative predictive value (NPV) was 72%. Likewise, the optimal threshold of RPSI to detect PAD was calculated to be 74 s^{-1} in the diabetic population, with a PPV of 91% and an NPV of 71%. In summary, compared to the traditional ABI method, the diagnostic PPV were increased by 22% using the ACCmax method and by 17% using the RPSI method. Furthermore, combining ACCmax and RPSI in a parallel test increased the diagnostic specificity to 95% in the diabetic population.

In a second study, a population of 25 PAD patients were enrolled, and 44 tibial arteries were evaluated before and after revascularisation. The average of ACCmax was 427.83 ± 171.67 cm/s^2 before revascularisation and 509.30 ± 171.23 cm/s^2 ($P = 0.002$) after revascularisation. The average of RPSI before revascularisation was 82.17 ± 58.76 s^{-1}, and it was 64.08 ± 39.65 s^{-1} after revascularisation. Both parameters demonstrated feasibility for monitoring PAD after revascularisation, which is promising in replacing ABI as a surveillance approach (5.3).

In the third part of the study, the dynamic changes of ACCmax and RPSI of carotis under ECP treatment were examined at different treatment pressures using 18 healthy volunteers. Under 0 mmHg, 80 mmHg and 160 mmHg treatment pressures, ACCmax were 1239.54 ± 20.40 cm/s^2, 1331.83 ± 12.85 cm/s^2 and 1329.92 ± 195.34 cm/s^2, respectively ($P < 0.05$), and RPSI were 41.67 ± 5.66 s^{-1}, 45.31 ± 7.12 s^{-1} and 48.72 ± 7.10 s^{-1}, respectively ($P < 0.05$). The haemodynamics of participants reacted differently on an individual basis to the increase of ECP pressure, and the maximal amplitude of diastolic ACCmax was approximately 200% of the base-level of diastolic ACCmax.

5.1 Validation of the Gefäßtachometer approach on peripheral arteries

Recurrent concerns regarding several 1D analysis models are the accuracy of model predictions and the physiological relevance of results. The focus of this study was the quantitative evaluation of waveforms and the calculation of initial acceleration and mean velocity to establish a fast screening test for distal blood perfusions. Therefore, the measurement models were designed and validated in three study populations: (1) PAD-unaffected patients, who had a standard arterial flow and haemodynamic characteristics; (2) PAD-affected patients, who had different ranges of vascular lesions; and (3) patients post-revascularisation and ECP intervention, who had dynamic changes in arterial flow. Because the study was designed to be a prospective diagnostic study and all relevant participants had a high risk for PAD, samples from PAD-unaffected patients were still affected by subclinical pathological alterations and could not be considered samples from healthy young adults. Thus, the study participants properly reflected the clinical situation.

A vascular-unaffected patient can be used as an example to demonstrate the analysis procedure in **Figure 6A**. The diagram shows good agreement between computational predictions and Doppler measurements. On the other hand, **Figure 6** shows that in the vascular pathological population (PAD patients in this study), the flow velocity patterns exhibit different alterations of the velocity signal, such as the delay of the acceleration slope, depression of the wave peak and extension of the systolic period. These ischemic characteristics were measured by a Doppler device and then translated into a computer-assisted mathematically lossless procedure (**Figure 6B, Figure 6C and Figure 6D**). Moreover, intra- and inter-individual differences of arterial flow adaption mechanisms were measured in patients after revascularisation or one-time ECP intervention. Whether the data were collected one day after intervention (revascularisation) or during real-time ECP treatment, the velocity patterns showed agreement between the measured curves and the computer-calculated curves under the condition that the wall properties were displayed correctly and clearly.

The basic and key issues for the application of ultrasounds in assessing ACCmax and RPSI depend on the accurate estimation of instantaneous maximum blood flow velocity waveforms in a large range of the frequencies. It is well-known that the instantaneously maximum blood flow velocity is proportional to the instantaneously maximal frequency (Fmax) of the Doppler frequency spectrum, and Fmax is obtained using the modified geometric method (MGM)[58]. Maximum Doppler frequency refers to the maximal vertical distance between the integrated spectrums and the reference line. Hence, the velocity curve was obtained using a computational

approach. In this study, the Gefäßtachometer programme was applied to MGM to estimate the maximum Doppler frequency.

The analogue signal of acceleration is not yet available in the current Doppler system, but as first proposed by Hanni NS et al.[69], it could be obtained through the external differentiation of the velocity waveform. With a time-resolution of 15ms and a moving average filter of a 3-point smoothing algorithm, the programme could calculate the instantaneous first derivative, or the instantaneous blood acceleration[70]. In this study, the ensemble-velocity curve procedure was performed before calculation, and the velocimetic values of the ensemble line were the mathematical average of each curve collected in 15s. Therefore, the inter-beat variability was reduced, and the accuracy of this technique was improved.

Utilising the Doppler ultrasound for the detection of PAD has been reviewed previously[61]. In a spectral Doppler waveform analysis, the normal waveform profile is triphasic. The first component resulting from the initial systolic forward flow. Next, in the early diastolic phase, there is a flow reversal reflecting the decreasing of left ventricular pressure before aortic valve closure. In the late diastole phase, a small amount of forward flow is the consequence of the vascular elastic recoil. In a pathological situation, on the one hand, the diastolic component of a normal triphasic signal is absent due to a stiff atherosclerotic change; on the other hand, the waveform shape is also determined by the blood flow resistance of distal arteries or the degree of dilation in the distal resistance arterioles. In the progression of PAD, long-time ischemia could lead to over-dilated arterioles distally on the feet and could cause increased susceptibility to amputation. In this study, severe ischemic Doppler signals were examined, and a further sub-classification was designed: the latter pathological situation demonstrates a signal similar to the waveform of an internal carotid artery and has a Vmax of less than 30 cm/s, which was sub-classified as a weak monophasic signal.

Therefore, the novel quantitative analysis method of pulsatile flow has an important complimentary role in the traditional Doppler system, which could be used to compute the haemodynamic characteristics of ACCmax and RPSI.

5.2 Diagnostic application in screening PAD patients

In light of the limitations of ABI for assessing PAD, the measurement of interior blood flow is a promising new concept. Due to its independence from vascular wall changes, the flow measurements are more precise than ABI. The 1D analysis-based flow measurement is much

easier to perform. While 3D methodologies have contributed to a large number of advancements, they require sophisticated methodologies and are time-consuming[71-73].

In 2006, the application of the quantification of systolic acceleration for detecting stenosis was first proposed in clinical research in the context of renal arterial stenosis[74]. This method was subsequently transferred to peripheral artery research in 2010[31]. These are breakthrough concepts; however, these methods are not yet widely used in the routine monitoring and assessment of arterial stenosis due to a number of limitations. First, the previous data collection process is dependent on the operator's experience, and the results vary due to the occasional increase of signal-to-noise ratio. Second, the detection of maximal acceleration is susceptible to artificial errors during the identification of slope outlines, which was remarkably improved through the computational output of Fmax and wave outlines. While the error between the visual and computed detection of ACCmax would be minimal in healthy vascular populations, the error would be relevant in the vascular disease population due to the delay of the slope in pathological states compared with healthy states. Third, due to the limitations of ABI, it is not reliable as a gold standard in a diagnostic study. Furthermore, ACCmax characterises the initial slope but neglects the haemodynamic information during the whole heartbeat, which has been repeatedly reviewed in recent literature[75-77].

All the aforementioned methodological pitfalls have been addressed in our study. The first two limitations were addressed through applying a computerised analogue (**Figure 5**). In this way, original Doppler signals were maintained at a maximal level, in comparison with signal loss during the pre-process of commonly commercial Doppler system. As for assessment of ACCmax and RPSI, a standard computerised process minimised the artificial error. For the third limitation, according the guideline[59], angiography was used as the gold standard in our study, as shown in **Figure 6**. The close accordance between our ACCmax values and the percentage of stenosis using angiography as well as the further considerable performance of the ROC analysis favoured the use of Doppler-derived ACCmax and RPSI to predict PAD and its degree. Similar to the study by Tongeren et al., we also performed the correlation analysis between ACCmax and ABI, but it turned out to be weak. On one hand, the weak correlation resulted from the different definitions of PAD from our study than the research of Tongeren et al. On the other hand, the weak correlation between ACCmax and ABI indicated that ACCmax and ABI were independent and non-substituent diagnostic tools because different aspects of haemodynamics are observed. For the last limitation, RPSI – by taking the Vmean of the systolic and diastolic phases into account – serves ingeniously as an additional parameter to ACCmax, even though RPSI solely

cannot make a diagnosis of PAD. For example, given two patients with similar ACCmax values but different Doppler waveform and mean flow velocity values, the slow and continuous forward flow could be discriminated via a low level of RPSI. This characteristic was in agreement with our group's finding in 2010 that RPSI could discriminate the pulsatility of arteries from veins[32], and the current study represents the first time that RPSI has been validated in real patients.

For diagnostic studies, an appropriate sample size is the premise for statistical efficiency. The sample size in this study was estimated according to a previous incidence of PAD, because from a statistical perspective, the incidence of disease plays an indispensable role in determining PPV and NPV. The proportion of PAD and non-PAD samples was approximately 1:1. The participants were recruited from a clinic vascular laboratory and met the criteria for high-risk factors. With an equivalence of 5% and a statistical power of more than 80%, it is reasonable to accept the sample size as representative of the entire potential population for vascular disease.

The distributions of ACCmax and RPSI had statistically significant differences between the non-PAD group and PAD group (**Figure 7**), which indicated their potential to serve as diagnostic parameters. The performance of ACCmax was in agreement with the research of Tongeren et al[31].

While the distributions of ACCmax were more clearly differentiated than that of RPSI, RPSI offered superior benefits in characterising different stages of PAD by identifying waveform subgroups. **Figure 8** shows that the RPSI values increased significantly when monophasic signals weakened, and the RPSI values decreased significantly when signals weakened further to weak monophasic signals and a continuous forward flow.

The weak correlation demonstrated in **Figure 9**, including the correlations between ACCmax and ABI and the correlation between RPSI and ABI, did not reduce the diagnostic reliability of ACCmax and RPSI. Contrarily, they indicated that new parameters of ACCmax and RPSI and traditional ABI were independent and non-substituent diagnostic tools because different aspects of haemodynamics were observed. Interestingly, in **Figure 9A** and **Figure 9B**, by observing the distributions of the scatters of two different colours, false-negative PAD determinations in the ABI range of > 1.3 as well as in the ABI range of 0.9-1.3 are shown, which occurred more frequently in the diabetic group. This observation is in agreement with previous acknowledgements about VCm. Considering the limitation of ABI, the TBI approach was also explored in our study. But as published in previous literatures[25], the performance of toe blood

pressure was not certain in our study. In total, in 44 arteries complicated with VCm, toe blood pressure was only available in 18 of them, while it failed to ascertain toe blood pressure measurements in the remaining 26 arteries. Due to the limited sample volume, statistical analysis was not performed.

Figure 10 demonstrates the acceptable accordance between the percentage of stenosis and the three new assessment parameters, ACCmax, RPSI and ACCmax-ratio; however, there is a concern that the association coefficients of R^2 were not significantly larger than 0.5. Angiography has been commonly recognised as the gold standard, but it does not reflect the haemodynamically functional situation. The assessment of ACCmax and RPSI in our study was obtained from distal tibial arteries, around the area of the ankle; thus, the values of ACCmax and RPSI are independent in terms of the locations of stenosis. But they demonstrated statistically significant correlation with the severity of stenosis. The correlation between ACCmax and stenosis percentage was at a moderate level, because in some individuals, the results of stenosis percentage and the functional parameters of ACCmax and RPSI were inverse. For instance, the observed monophasic waveforms could result from one haemodynamically relevant stenosis or multiple non-significant atherosclerotic lesions, since blood flow waves attenuated gradually to a monophasic pattern and diminished the second and third wave components. On the other hand, due to collateral perfusion, proximal occlusion or stenosis of the femoral artery could develop into a triphasic signal on a Doppler examination of distal tibial arteries. This highlights the significance of evaluating blood perfusion from the distal tibial arteries, since the functional net of forward perfusion is a concern.

For comparing the diagnostic performance of various parameters and thus calculating the threshold values, an ROC method was applied in which the principle was AUC, and the best threshold was calculated based on the ultimate point, graphically, on the curve to the chance line. The diagnostic performance of ACCmax was better than that of RPSI, as the AUC of the former was higher (**Figure 11** and **Figure 12**). The double cut-off values with either a sensitivity of 90% or a specificity of 90%, which were found by Tongeren et al[31], were also reproduced in this study; however, the issue involving the grey zone could not be avoided. When using the criteria of either ACCmax or RPSI, the determination was based on one characteristic of internal flow. In theory, a more accurate prediction would be obtained by combining the advantage of the indices of ACCmax, RPSI and ABI. As mentioned, the advantages of RPSI include its assistance in differentiating between the stages of PAD. Therefore, three types of combing models were used, which are widely accepted in the statistical area of estimating the diagnostic performance.

First, the logistic regression (**Figure 13**) in which one logistic parameter was calculated based on the parameters of the ACCmax and ABI of each individual was investigated. Unfortunately, this simple mathematic combination did not make full use of the characteristics of each parameter; thus, the diagnostic performance of the logistic regression failed to improve significantly compared to a single parameter (ACCmax, RPSI or ABI). The AUC of the logistic regression was 87%, while the AUC of ACCmax was 85%.

Second, the parallel test in **Figure 14** was investigated, which was used to identify patients with either ACCmax of > 444 cm/s^2 or RPSI of > 58 s^{-1}, both of which were the thresholds calculated using the ROC method of each parameter. On one hand, the parallel test maintained the high specificity of ACCmax (98%) and RPSI (95%), which was much higher than that of ABI (83%) and the logistic regression (84%). On the other hand, using the parallel test showed a sensitivity of 68%, while both ACCmax and RPSI had previously failed to demonstrate a sensitivity > 60%.

Unfortunately, the sensitivity had not yet improved to more than 80%. Therefore, the data mining method, or decision tree, was examined. It can be observed in **Figure 16** that the determination of PAD was achieved through 5 layers of cut-off values by stepping forward into one layer after another layer. The behaviours of this network were characterised by the computational properties and the connections between them, similar to the synapses of the neurons, which is the reason that the technique is called ‘machine learning’. The weight of each synapse was determined in a complex series of mathematic equations, but once the parameters of ACCmax, RPSI and ABI were included, the output of the PAD diagnosis could be obtained. Hence, different haemodynamic features were captured as often as possible. Not surprisingly, the sensitivity increased to 88%. Therefore, integrating the computational measurement technique and computational determination technique are promising in obtaining a computational diagnosis.

In addition, high values of ACCmax (> 1000 cm/s^2) were frequently observed in the ABI range > 1.3 (shown in **Figure 9**), which implicated the existence of VCm. Due to the correlated mathematic and physiological principles, it was assumed that high values of ACCmax were proportional to high values of pulse wave velocity (PWV) and thus the coexistence of VCm.

The blood pressure and flow waves can be divided into their respective forward and backward components. The forward wave originates from the ejection of the heart and travels to the peripheral arterioles, while the backward wave develops due to a large mismatch between terminal impedances. It is widely known that in VCm, the increase of PWV results from the

combination of the reflected wave to the forward wave, leading to a higher pressure peak in the late systolic phase compared to normal healthy wave patterns[68, 78] (**Figure 19**). Further observations by Jonathan et al.[78] showed that this reflected wave could expand forward again and form a re-reflection wave. Thus, it coincides with the mid-systolic forward wave. In other words, in cases of VCm, the pressure waveforms of the upstream as well as the waveforms of the downstream are transformed due to the addition of the reflected wave, demonstrating as the sharp slope of pressure waveform in **Figure 19**.

Coming back to our study, velocimetic parameters were observed, including ACCmax, RPSI and mean velocity. According to Newton's second law of motion ($F = m * a$) and Ohm's law ($F = \frac{\Delta p}{R}$), we could develop $a = \frac{\Delta p}{R * m}$. In this formula, ΔP is the local blood pressure gradient, R is the local blood resistance, m is the mass of local blood and a is the blood acceleration. Thus, for a given blood resistance and given blood mass, acceleration is derived from the instantaneous maximal derivative of arterial pressure (Δp). Therefore, the observations of the sharp increase of systolic velocity waveforms and high values of ACCmax in our study was similar to sharp increase of blood pressure waveform shown in **Figure 19**. Unfortunately, the approach of PWV [17, 68] and thus the verification of VCm were not included in this study.

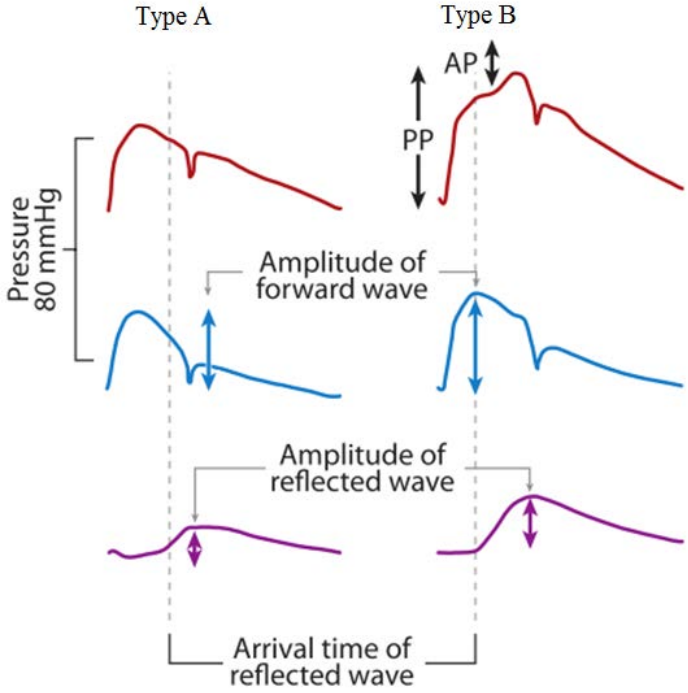

Figure 19 The pressure waves in a young (type A) and older (type B) men and the corresponding forward and backward components. AP represents a pronounced late systolic peak while PP means the pulse pressure (Taken from Westerhof et al. in 2005).

5.3 Advantages of post-intervention controlling

The long-term patency rate of percutaneous angioplasty and stenting in the lower extremities were observed to be 50%–85% in recent studies[61]. For surveillance, a follow-up analysis of the ankle blood pressure was recommended by ESC guidelines in 2011[59]; however, a systematic duplex surveillance program was not found to be beneficial in terms of graft patency rates or limb survival rates[79]. Therefore, a consensual protocol for revascularisation surveillance is needed[80].

In this study, in comparison with the unstable performance of ABI values after revascularisation (not shown due to frequent inaccessibility), corresponding acute haemodynamic improvements of ACCmax and RPSI were observed (**Table 4**). To understand the vascular behaviours behind the increasing of these two parameters, two important types of blood flow adaptation mechanisms should be considered[68]. The first mechanism is the autoregulation of the microcirculation, which is determined by the metabolic needs or by local mechanical environment changes. For PAD, after long-term adaptation to the distal ischemia, peripheral resistance of one or more relevant arterioles decreases[81]. In this way, the local haemodynamic situations as well as velocimetic parameters were compensated to some extent but still below the normal values. Second, flow-induced vascular dilatation leads to the decrease of local vascular smooth muscle tone and endothelium-dependent vaso-relaxation. Thus, large vessels may exhibit increasing compliance as a form of short-term adaption[68]. Consequently, distal haemodynamic situation would be increased, which would be reflected as the improvement of the velocimetic parameters after revascularisation.

In addition, it was observed that the lower the basic levels of ACCmax and RPSI were, the more clearly these values improved after revascularisation (**Figure 17**), which indicated more improvement in the blood perfusion of the distal ankle area. Recent studies have shown that the revascularisation patency is dependent on anatomic reconstruction as well as the improvement of blood perfusion in the distal ankle area[62]. Patients suffering from more severe blood flow deficits in the distal ankle area have an increased risk for amputation[11]. Therefore, by quantitatively demonstrating the improvement of distal blood flow, the novel surveillance approach with ACCmax and RPSI could help predict the likelihood of receiving benefits from revascularisation as well as the risk for amputation.

Interestingly, inverse tendencies were observed for ACCmax and RPSI: ACCmax values increased significantly after revascularisation, while RPSI decreased significantly after

revascularisation. This occurred because the extent of the increase of velocity was superior to the extent of the increase of ACCmax after revascularization. But as for the reason why Vmean increased more intensively than RPSI was not total clearly understand.

5.4 The applicability of modulating ACCmax and RPSI-derived FSS under ECP pressure

In the first and second part of the study, it was proven that ACCmax and RPSI could serve as diagnostic indices and could provide surveillance information. The aim of the third part of the study was to analyse flow velocimetic parameters under the sessions of ECP treatment using a real-time dynamic analysis of carotis in healthy volunteers.

Unfortunately, clear tendencies of ACCmax or RPSI were not observed in all 18 volunteers, as shown in **Table 6**; however, when evaluating the dynamics of the systolic ACCmax of each individual, a maximal increasing magnitude of 200% was observed in nine volunteers (50%), as shown in **Figure 18**. Interestingly, the target ECP pressure values, which demonstrated a 200% increase in systolic ACCmax, were not alike among individuals. The assumption of a 200% increase in systolic accelerations is not uncommon. In another ECP-assisted PAD treatment study, a 200% increase of systolic acceleration was also proposed in PAD patients under low ECP pressure treatment (140–160 mmHg)[82]. This shows that a patient individual analysis of the hemodynamic situation is relevant for assessing the optimal treatment pressure.

Due to the correlation between the velocimetic parameters and FSS, a 200% increase in ACCmax indicated a 200% increase in the maximal change rate of FSS divided by time-average FSS. FSS is the driving force of arteriogenesis, which is the remodelling of pre-existing collateral arteries to form functional conductance arteries[83,84]. Formerly, research on FSS-related arteriogenesis has been inconsistent, and one of the reasons was the lack of a reproducible intervention procedure. In this study, the applicability of a combing ECP device and of the measurements of ACCmax and RPSI is shown. Therefore, a novel approach to modulate FSS and to obtain feedback of haemodynamic values in real time is provided; however, one limitation of the study was that collateral growth was not observed, and thus the pathophysiological effect of this ACCmax and RPSI-based modulation of FSS is uncertain.

6 Conclusion

This work presents the following results of the three-part study:

First, the diagnostic thresholds of PAD in diabetic populations were observed: ACCmax of 444 cm/s^2 and RPSI of 57 s^{-1}. The diagnostic specificity of each parameter was more than 95%, while the diagnostic sensitivity of each parameter was less than 60%. Using the combination model of a decision tree, the sensitivity was increased to 88%.

Second, the new parameters of ACCmax and RPSI were significantly improved ($P < 0.05$) one day after revascularisation, and the patients suffering from more severe PAD demonstrated obvious improvements in ACCmax and RPSI.

Third, the real-time measurement of ACCmax and RPSI were observed under ECP treatment from the carotis of 18 healthy volunteers. The increase of the systolic ACCmax could be up to 200%. Therefore, the applicability of the combing ECP device and of the measurements of ACCmax and RPSI has been proven, and thus a novel approach to modulate FSS and to obtain feedback of haemodynamic values in real time has been developed.

Using the Gefäßtachometers technique, the RPSI and ACCmax measurement provided a more predictive diagnosis than ABI for estimating the PAD status of diabetic patients. The digital translation of Doppler signals and the computer-assisted calculation of haemodynamics served as essential technical foundations for future computer-aided PAD diagnoses; however, the combination model of the decision tree requires a broader study in the future. Using ACCmax and RPSI for PAD surveillance and individual ECP treatment is now possible, but multi-centred studies are still needed due to the small number of patients in the study.

Bibliography

1. Ouriel K. Peripheral arterial disease. *The lancet*. 2001;358:1257-1264.

2. Meijer WT, Hoes AW, Rutgers D, Bots ML, Hofman A and Grobbee DE. Peripheral Arterial Disease in the Elderly The Rotterdam Study. *Arteriosclerosis, thrombosis, and vascular biology*. 1998;18:185-192.

3. Fowkes F, Housley E, Cawood E, Macintyre C, Ruckley C and Prescott R. Edinburgh Artery Study: prevalence of asymptomatic and symptomatic peripheral arterial disease in the general population. *International journal of epidemiology*. 1991;20:384-392.

4. Reinecke H, Unrath M, Freisinger E, Bunzemeier H, Meyborg M, Lüders F, Gebauer K, Roeder N, Berger K and Malyar NM. Peripheral arterial disease and critical limb ischaemia: still poor outcomes and lack of guideline adherence. *European heart journal*. 2015:ehv006.

5. Holman N, Young R and Jeffcoate W. Variation in the recorded incidence of amputation of the lower limb in England. *Diabetologia*. 2012;55:1919-1925.

6. Joosten MM, Pai JK, Bertoia ML, Rimm EB, Spiegelman D, Mittleman MA and Mukamal KJ. Associations between conventional cardiovascular risk factors and risk of peripheral artery disease in men. *JAMA*. 2012;308:1660-1667.

7. Criqui MH and Aboyans V. Epidemiology of peripheral artery disease. *Circulation research*. 2015;116:1509-1526.

8. Aboyans V, Lacroix P, Tran M-H, Salamagne C, Galinat S, Archambeaud F, Criqui MH and Laskar M. The prognosis of diabetic patients with high ankle-brachial index depends on the coexistence of occlusive peripheral artery disease. *Journal of vascular surgery*. 2011;53:984-991.

9. Guo X, Shi Y, Huang X, Ye M, Xue G and Zhang J. Features analysis of lower extremity arterial lesions in 162 diabetes patients. *Journal of Diabetes Research*. 2013;2013.

10. Martí X, Romera A, Vila R and Cairols MA. Role of ultrasound arterial mapping in planning therapeutic options for critical ischemia of lower limbs in diabetic patients. *Annals of vascular surgery*. 2012;26:1071-1076.

11. Tsai C-Y, Chu S-Y, Wen Y-W, Hsu L-A, Chen C-C, Peng S-H, Huang C-H, Sun J-H and Huang Y-Y. The value of Doppler waveform analysis in predicting major lower extremity amputation among dialysis patients treated for diabetic foot ulcers. *Diabetes research and clinical practice*. 2013;100:181-188.

12. Weinberg I, Giri J, Calfon MA, Hawkins BM, Weinberg MD, Margey R, Hannon K, Schainfeld RM and Jaff MR. Anatomic correlates of supra‐normal ankle brachial indices. *Catheterization and Cardiovascular Interventions*. 2013;81:1025-1030.

13. Zhang H, Li X-Y, Si Y-j, Lu X-l, Luo X-S and Liu Z-y. Manifestation of lower extremity atherosclerosis in diabetic patients with high ankle-brachial index. *Chinese medical journal*. 2010;123:890-894.

14. Leeper NJ, Myers J, Zhou M, Nead KT, Syed A, Kojima Y, Caceres RD and Cooke JP. Exercise capacity is the strongest predictor of mortality in patients with peripheral arterial disease. *Journal of vascular surgery*. 2013;57:728-733.

15. Golomb BA, Dang TT and Criqui MH. Peripheral arterial disease morbidity and mortality implications. *Circulation*. 2006;114:688-699.

16. Conte MS, Pomposelli FB, Clair DG, Geraghty PJ, McKinsey JF, Mills JL, Moneta GL, Murad MH, Powell RJ and Reed AB. Society for Vascular Surgery practice guidelines for atherosclerotic occlusive disease of the lower extremities: Management of asymptomatic disease and claudication. *Journal of vascular surgery*. 2015;61:2S-41S.

17. Lanzer P, Boehm M, Sorribas V, Thiriet M, Janzen J, Zeller T, St Hilaire C and Shanahan C. Medial vascular calcification revisited: review and perspectives. *European heart journal*. 2014:ehu163.

18. Niskanen L, Siitonen O, Suhonen M and Uusitupa MI. Medial artery calcification predicts cardiovascular mortality in patients with NIDDM. *Diabetes care*. 1994;17:1252-1256.

19. Lehto S, Niskanen L, Suhonen M, Rönnemaa T and Laakso M. Medial artery calcification a neglected harbinger of cardiovascular complications in non–insulin-dependent diabetes mellitus. *Arteriosclerosis, thrombosis, and vascular biology*. 1996;16:978-983.

20. London GM, Guérin AP, Marchais SJ, Métivier F, Pannier B and Adda H. Arterial media calcification in

end-stage renal disease: impact on all-cause and cardiovascular mortality. *Nephrology Dialysis Transplantation*. 2003;18:1731-1740.

21. Glagov S, Weisenberg E, Zarins CK, Stankunavicius R and Kolettis GJ. Compensatory enlargement of human atherosclerotic coronary arteries. *New England Journal of Medicine*. 1987;316:1371-1375.

22. van Varik BJ, Rennenberg RJ, Reutelingsperger CP, Kroon AA, de Leeuw PW and Schurgers LJ. Mechanisms of arterial remodeling: lessons from genetic diseases. *Frontiers in genetics*. 2012;3.

23. Suominen V, Rantanen T, Venermo M, Saarinen J and Salenius J. Prevalence and risk factors of PAD among patients with elevated ABI. *European Journal of Vascular and Endovascular Surgery*. 2008;35:709-714.

24. Aboyans V, Criqui MH, Abraham P, Allison MA, Creager MA, Diehm C, Fowkes FGR, Hiatt WR, Jönsson B and Lacroix P. Measurement and Interpretation of the Ankle-Brachial Index A Scientific Statement From the American Heart Association. *Circulation*. 2012;126:2890-2909.

25. Tehan PE, Bray A and Chuter VH. Non-invasive vascular assessment in the foot with diabetes: sensitivity and specificity of the ankle brachial index, toe brachial index and continuous wave Doppler for detecting peripheral arterial disease. *Journal of diabetes and its complications*. 2016;30:155-160.

26. Sahli D, Eliasson B, Svensson M, Blohmé G, Eliasson M, Samuelsson P, Öjbrandt K and Eriksson JW. Assessment of toe blood pressure is an effective screening method to identify diabetes patients with lower extremity arterial disease. *Angiology*. 2004;55:641-651.

27. Williams DT, Harding KG and Price P. An evaluation of the efficacy of methods used in screening for lower-limb arterial disease in diabetes. *Diabetes care*. 2005;28:2206-2210.

28. Tehan PE, Santos D and Chuter VH. A systematic review of the sensitivity and specificity of the toe–brachial index for detecting peripheral artery disease. *Vascular Medicine*. 2016:1358863X16645854.

29. Decrinis M, Doder S, Stark G and Pilger E. A prospective evaluation of sensitivity and specificity of the ankle/brachial index in the follow-up of superficial femoral artery occlusions treated by angioplasty. *The Clinical investigator*. 1994;72:592-7.

30. Radak D, Labs KH, Jager KA, Bojic M and Popovic AD. Doppler-based diagnosis of restenosis after femoropopliteal percutaneous transluminal angioplasty: sensitivity and specificity of the ankle/brachial pressure index versus changes in absolute pressure values. *Angiology*. 1999;50:111-22.

31. Van Tongeren R, Bastiaansen A, Van Wissen R, Le Cessie S, Hamming J and Van Bockel J. A comparison of the Doppler-derived maximal systolic acceleration versus the ankle-brachial pressure index or detecting and quantifying peripheral arterial occlusive disease in diabetic patients. *The Journal of cardiovascular surgery*. 2010;51:391-398.

32. Buschmann I, Pries A, Styp-Rekowska B, Hillmeister P, Loufrani L, Henrion D, Shi Y, Duelsner A, Hoefer I, Gatzke N, Wang H, Lehmann K, Ulm L, Ritter Z, Hauff P, Hlushchuk R, Djonov V, van Veen T and le Noble F. Pulsatile shear and Gja5 modulate arterial identity and remodeling events during flow-driven arteriogenesis. *Development*. 2010;137:2187-96.

33. Malek AM, Alper SL and Izumo S. Hemodynamic shear stress and its role in atherosclerosis. *Jama*. 1999;282:2035-2042.

34. Stone PH, Saito S, Takahashi S, Makita Y, Nakamura S, Kawasaki T, Takahashi A, Katsuki T, Nakamura S and Namiki A. Prediction of progression of coronary artery disease and clinical outcomes using vascular profiling of endothelial shear stress and arterial plaque characteristics: the PREDICTION Study. *Circulation*. 2012:CIRCULATIONAHA. 112.096438.

35. Kwak BR, Bäck M, Bochaton-Piallat M-L, Caligiuri G, Daemen MJ, Davies PF, Hoefer IE, Holvoet P, Jo H and Krams R. Biomechanical factors in atherosclerosis: mechanisms and clinical implications. *European heart journal*. 2014:ehu353.

36. Schuler G, Adams V and Goto Y. Role of exercise in the prevention of cardiovascular disease: results, mechanisms, and new perspectives. *European heart journal*. 2013;34:1790-1799.

37. Wilson MG, Ellison GM and Cable NT. Basic science behind the cardiovascular benefits of exercise. *Heart*. 2015;101:758-765.

38. Padilla J, Johnson BD, Newcomer SC, Wilhite DP, Mickleborough TD, Fly AD, Mather KJ and Wallace JP. Normalization of flow-mediated dilation to shear stress area under the curve eliminates the impact of variable hyperemic stimulus. *Cardiovasc Ultrasound*. 2008;6:42.

39. Pyke KE, Dwyer EM and Tschakovsky ME. Impact of controlling shear rate on flow-mediated dilation responses in the brachial artery of humans. *Journal of Applied Physiology*. 2004;97:499-508.

40. Betik AC, Luckham VB and Hughson RL. Flow-mediated dilation in human brachial artery after different circulatory occlusion conditions. *American Journal of Physiology-Heart and Circulatory Physiology*. 2004;286:H442-H448.

41. Stoner L and Sabatier MJ. Use of ultrasound for non-invasive assessment of flow-mediated dilation. *Journal of atherosclerosis and thrombosis*. 2012;19:407-421.

42. Cho YI, Cho DJ and Rosenson RS. Endothelial Shear Stress and Blood Viscosity in Peripheral Arterial Disease. *Current atherosclerosis reports*. 2014;16:1-10.

43. Thijssen DH, Dawson EA, Tinken TM, Cable NT and Green DJ. Retrograde flow and shear rate acutely impair endothelial function in humans. *Hypertension*. 2009;53:986-992.

44. Tinken TM, Thijssen DH, Hopkins N, Black MA, Dawson EA, Minson CT, Newcomer SC, Laughlin MH, Cable NT and Green DJ. Impact of shear rate modulation on vascular function in humans. *Hypertension*. 2009;54:278-285.

45. Hoi Y, Zhou Y-Q, Zhang X, Henkelman RM and Steinman DA. Correlation between local hemodynamics and lesion distribution in a novel aortic regurgitation murine model of atherosclerosis. *Annals of biomedical engineering*. 2011;39:1414-1422.

46. Chiu J-J and Chien S. Effects of disturbed flow on vascular endothelium: pathophysiological basis and clinical perspectives. *Physiological reviews*. 2011;91:327-387.

47. White CR, Haidekker M, Bao X and Frangos JA. Temporal gradients in shear, but not spatial gradients, stimulate endothelial cell proliferation. *Circulation*. 2001;103:2508-2513.

48. Hsiai TK, Cho SK, Honda HM, Hama S, Navab M, Demer LL and Ho C-M. Endothelial cell dynamics under pulsating flows: significance of high versus low shear stress slew rates ($\partial \tau/\partial \tau$). *Annals of biomedical engineering*. 2002;30:646-656.

49. Apodaca G. Modulation of membrane traffic by mechanical stimuli. *American Journal of Physiology-Renal Physiology*. 2002;282:F179-F190.

50. Barakat AI and Lieu DK. Differential responsiveness of vascular endothelial cells to different types of fluid mechanical shear stress. *Cell biochemistry and biophysics*. 2003;38:323-343.

51. Cullen JP, Sayeed S, Sawai RS, Theodorakis NG, Cahill PA, Sitzmann JV and Redmond EM. Pulsatile Flow–Induced Angiogenesis Role of Gi Subunits. *Arteriosclerosis, thrombosis, and vascular biology*. 2002;22:1610-1616.

52. Ashor AW, Lara J, Siervo M, Celis-Morales C, Oggioni C, Jakovljevic DG and Mathers JC. Exercise modalities and endothelial function: a systematic review and dose–response meta-analysis of randomized controlled trials. *Sports Medicine*. 2015;45:279-296.

53. Greyling A, Schreuder TH, Landman T, Draijer R, Verheggen RJ, Hopman MT and Thijssen DH. Elevation in blood flow and shear rate prevents hyperglycemia-induced endothelial dysfunction in healthy subjects and those with type 2 diabetes. *Journal of Applied Physiology*. 2015;118:579-585.

54. Halliwill JR, Buck TM, Lacewell AN and Romero SA. Postexercise hypotension and sustained postexercise vasodilatation: what happens after we exercise? *Experimental physiology*. 2013;98:7-18.

55. Michaels AD, Accad M, Ports TA and Grossman W. Left ventricular systolic unloading and augmentation of intracoronary pressure and Doppler flow during enhanced external counterpulsation. *Circulation*. 2002;106:1237-1242.

56. Jeevanantham V, Chehab B, Austria E, Shrivastava R, Wiley M, Tadros P, Dawn B, Vacek JL and Gupta K. Comparison of accuracy of two different methods to determine ankle-brachial index to predict peripheral arterial disease severity confirmed by angiography. *Am J Cardiol*. 2014;114:1105-10.

57. Nead KT, Cooke JP, Olin JW and Leeper NJ. Alternative ankle-brachial index method identifies additional at-risk individuals. *J Am Coll Cardiol*. 2013;62:553-9.

58. Fernando KL, Mathews VJ and Clark EB. A mathematical basis for the application of the modified geometric method to maximum frequency estimation. *Biomedical Engineering, IEEE Transactions on*. 2004;51:2085-2088.

59. Tendera M, Aboyans V, Bartelink M-L, Baumgartner I, Clément D, Collet J-P, Cremonesi A, De Carlo M, Erbel R and Fowkes FGR. ESC Guidelines on the diagnosis and treatment of peripheral artery diseases Document covering atherosclerotic disease of extracranial carotid and vertebral, mesenteric, renal, upper and lower extremity arteriesThe Task Force on the Diagnosis and Treatment of Peripheral Artery Diseases of the European Society of Cardiology (ESC). *European heart journal*. 2011;32:2851-2906.

60. Reiber JH, Tu S, Tuinenburg JC, Koning G, Janssen JP and Dijkstra J. QCA, IVUS and OCT in interventional cardiology in 2011. *Cardiovascular diagnosis and therapy*. 2011;1:57.

61. Gerhard-Herman M, Gardin JM, Jaff M, Mohler E, Roman M and Naqvi TZ. Guidelines for noninvasive vascular laboratory testing: a report from the American Society of Echocardiography and the Society of Vascular Medicine and Biology. *Journal of the American Society of Echocardiography*. 2006;19:955-972.

62. Brownrigg J, Schaper N and Hinchliffe R. Diagnosis and assessment of peripheral arterial disease in the diabetic foot. *Diabetic Medicine*. 2015;32:738-747.

63. Spronk S, den Hoed PT, de Jonge LC, van Dijk LC and Pattynama PM. Value of the duplex waveform at the common femoral artery for diagnosing obstructive aortoiliac disease. *Journal of vascular surgery*. 2005;42:236-242.

64. Donnelly R, Hinwood D and London NJ. Non-invasive methods of arterial and venous assessment. *British Medical Journal*. 2000;320:698.

65. Nallamothu BK, Spertus JA, Lansky AJ, Cohen DJ, Jones PG, Kureshi F, Dehmer GJ, Drozda JP, Walsh MN and Brush JE. Comparison of clinical interpretation with visual assessment and quantitative coronary angiography in patients undergoing percutaneous coronary intervention in contemporary practice: the Assessing Angiography (A2) project. *Circulation*. 2013:CIRCULATIONAHA. 113.001952.

66. Matsukura M, Hoshina K, Shigematsu K, Miyata T and Watanabe T. Paramalleolar Arterial Bollinger Score in the Era of Diabetes and End-Stage Renal Disease–Usefulness for Predicting Operative Outcome of Critical Limb Ischemia–. *Circulation Journal*. 2015.

67. Forsythe R, Brownrigg J and Hinchliffe R. Peripheral arterial disease and revascularization of the diabetic foot. *Diabetes, Obesity and Metabolism*. 2015;17:435-444.

68. van de Vosse FN and Stergiopulos N. Pulse wave propagation in the arterial tree. *Annual Review of Fluid Mechanics*. 2011;43:467-499.

69. Sabbah HN, Khaja F, Brymer JF, McFarland TM, Albert DE, Snyder JE, Goldstein S and Stein PD. Noninvasive evaluation of left ventricular performance based on peak aortic blood acceleration measured with a continuous-wave Doppler velocity meter. *Circulation*. 1986;74:323-329.

70. Chemla D, Levenson J, Valensi P, LeCarpentier Y, Pourny J-C, Pithois-Merli I and Simon A. Effect of beta adrenoceptors and thyroid hormones on velocity and acceleration of peripheral arterial flow in hyperthyroidism. *The American journal of cardiology*. 1990;65:494-500.

71. Wentzel JJ, Chatzizisis YS, Gijsen FJ, Giannoglou GD, Feldman CL and Stone PH. Endothelial shear stress in the evolution of coronary atherosclerotic plaque and vascular remodelling: current understanding and remaining questions. *Cardiovascular research*. 2012:cvs217.

72. Frauenfelder T, Boutsianis E, Schertler T, Husmann L, Leschka S, Poulikakos D, Marincek B and Alkadhi H. In-vivo flow simulation in coronary arteries based on computed tomography datasets: feasibility and initial results. *European radiology*. 2007;17:1291-1300.

73. Ramkumar PG, Mitsouras D, Feldman CL, Stone PH and Rybicki FJ. New advances in cardiac computed tomography. *Current opinion in cardiology*. 2009;24:596-603.

74. Bardelli M, Veglio F, Arosio E, Cataliotti A, Valvo E and Morganti A. New intrarenal echo-Doppler velocimetric indices for the diagnosis of renal artery stenosis. *Kidney international*. 2006;69:580-587.

75. Schreuder TH, Green DJ, Hopman MT and Thijssen DH. Impact of retrograde shear rate on brachial and superficial femoral artery flow-mediated dilation in older subjects. *Atherosclerosis*. 2015.

76. Schmitter S. The impact of chronic isolated increases in superficial femoral artery shear stress on flow-mediated dilation. 2015.

77. Ade CJ, Brown MG, Ederer AK, Hardy RN, Reiter LK and Didier KD. Influence of prior anterograde shear rate exposure on exercise‐induced brachial artery dilation. *Physiological reports*. 2015;3:e12414.

78. Mynard JP and Smolich JJ. One-Dimensional Haemodynamic Modeling and Wave Dynamics in the Entire Adult Circulation. *Annals of biomedical engineering*. 2015:1-18.

79. Davies A, Hawdon A, Sydes M and Thompson S. Is duplex surveillance of value after leg vein bypass grafting? Principal results of the Vein Graft Surveillance Randomised Trial (VGST). *Circulation*. 2005;112:1985-1991.

80. Bandyk DF. Surveillance after lower extremity arterial bypass. *Perspectives in vascular surgery and endovascular therapy*. 2007;19:376-383.

81. Alastruey J, Moore S, Parker K, David T, Peiró J and Sherwin S. Reduced modelling of blood flow in the cerebral circulation: coupling 1-D, 0-D and cerebral auto-regulation models. *International journal for numerical methods in fluids*. 2008;56:1061.

82. Buschmann EE, Brix M, Li L, Doreen J, Zietzer A, Li M, Buschmann I and Hillmeister P. Adaptation of external counterpulsation based on individual shear rate therapy improves endothelial function and claudication distance in peripheral artery disease. *VASA Zeitschrift fur Gefasskrankheiten*. 2016;45:317-24.

83. Yang D-y and Wu G-f. Vasculoprotective properties of enhanced external counterpulsation for coronary artery disease: Beyond the hemodynamics. *International journal of cardiology*. 2013;166:38-43.

84. Buschmann E, Utz W, Pagonas N, Schulz‐Menger J, Busjahn A, Monti J, Maerz W, Le Noble F, Thierfelder L and Dietz R. Improvement of fractional flow reserve and collateral flow by treatment with external counterpulsation (Art. Net.‐2 Trial). *European journal of clinical investigation*. 2009;39:866-875.

Affidavit

“I, [Lulu, Li] certify under penalty of perjury by my own signature that I have submitted the thesis on the topic [Measuring fluid shear stress with a novel Doppler-derived relative pulse slope index and maximal systolic acceleration approach to detect peripheral arterial disease and to modulate arteriogenesis]. I wrote this thesis independently and without assistance from third parties, I used no other aids than the listed sources and resources.

All points based literally or in spirit on publications or presentations of other authors are, as such, in proper citations (see "uniform requirements for manuscripts (URM)" the ICMJE www.icmje.org) indicated. The sections on methodology (in particular practical work, laboratory requirements, statistical processing) and results (in particular images, graphics and tables) correspond to the URM (s.o) and are answered by me. My interest in any publications to this dissertation correspond to those that are specified in the following joint declaration with the responsible person and supervisor. All publications resulting from this thesis and which I am author correspond to the URM (see above) and I am solely responsible.

The importance of this affidavit and the criminal consequences of a false affidavit (section 156,161 of the Criminal Code) are known to me and I understand the rights and responsibilities stated therein.

Date_____ Signature _____

Declaration of any eventual publications

[Lulu Li] had the following share in the following publications:

Publication 1: [Buschmann E., Brix M., **Li L.**, Janke D., Zietzer A., Li M., Buschmann I., Hillmeister P.], [A Novel Therapeutic Approach for Patients with Peripheral Artery Disease - Individual Shear Rate Therapy (ISRT)], [VASA], [2016]

Publication 2: [Zietzer A., Buschmann E., Janke D., **Li L.**, Brix M., Jungk C., Buschmann I., Hillmeister P.], [Acute physical exercise and long-term individual shear rate treatment increase telomerase activity in circulating leukocytes], [acta physiologica], [2016]

Signature, date and stamp of the supervising University teacher

_____

Signature of the doctoral candidate

_____

Curriculum Vitae / Lebenslauf

Lulu Li (cand.med)

My curriculum vitae does not appear in the electronic version of my paper for reasons of data protection.

Publikationsliste und Kongressbeiträge

My curriculum vitae does not appear in the electronic version of my paper for reasons of data protection.

Acknowledgement

The writing of this medical dissertation has been a precious journey in my academic life. I could not have travelled this far without the passionate and continued support of my advisors, colleagues, and family during these years of study in Berlin.

First and foremost, I would like to express my heartfelt gratitude to Professor Dr. Ivo Buschmann, my main advisor and supervisor, for the golden opportunity to perform my doctoral thesis at his department in Charité Universitätsmedizin Berlin. Meanwhile, I want to express my sincere gratitude to Mrs. Dr. Eva Buschmann for offering the opportunity and providing excellent guidance, encouragement, and care throughout the entire period of my study. Her mindful ideas and gentle words have enormous influence on me, not only on my study but also on my future life.

Second, I am thankful to Dr. Philipp Hillmeister for his initial encouragement for me to design the project and apply for the national scholarship. Furthermore, during these years' scientific training of speaking and writing with him, I experienced the wonderful feeling of science, which has never came to me before.

In addition, I am grateful to all members and colleagues from the research groups of Prof. Dr. Buschmann. I am deeply moved by Dr. Meijing Li by her kind and effective suggestions in academic life as well as in daily life. And I'm also grateful to Dr. Andreas Zietzer, Dr. Michèle Brix, and Dr. Doreen Jungk, who shared their wonderful experiences with me. I highly appreciate the statistical assistance from Dr. Andreas Busjahn over the last period of my study.

I am grateful for financial support from the China Scholarship Council.

Finally, special thanks belong to my husband Mr. Jing and my parents. Their continuous love and belief supported me the most for these three years. Without their love and support, I can never achieve all these.